iScience

CellPress
OPEN ACCESS

Review

Triboelectric nanogenerator: from alternating current to direct current

Di Liu,[1,2,4] Linglin Zhou,[1,2,4] Zhong Lin Wang,[1,2,3,*] and Jie Wang[1,2,*]

SUMMARY

Triboelectric nanogenerator (TENG) is considered as a potential solution to harvest distributed energy for the sustainable and reliable power supply of the internet of things. Although numerous researches on alternating current (AC) output TENG from fundamental physics to potential applications have been widely promoted in recent years, the studies about direct current (DC) output TENG is just beginning, especially for a constant current output. This work gives the summary of recent key researches from AC-TENG to DC-TENG, especially a constant current TENG, as well as the design of AC/DC-TENG. In addition, some new DC generators will also be summarized toward a wide range of readers. This study presents the similarities and differences between AC-TENG and DC-TENG, so that their impact and uniqueness can be clearly understood. Finally, the major challenges and the future outlooks in this rapidly emerging research field will be discussed as a guideline for future research.

INTRODUCTION

Development of electric energy

History and significance

From the discovery of electricity in antiquity such as triboelectrification (TE) effect in nature before BC 2600 to the wide applications of electric energy in the recent hundreds of years, the development of electric energy greatly accelerates the advancement and prosperity of human society. Especially in the recent hundreds of years, a great number of studies about electricity have been processed and people really understand how to utilize electricity, such as the famous experiment from Benjamin Franklin, performed with electricity drawn from thunderclouds, which greatly brought about widespread attention of electricity throughout the whole world. In 1831, Michael Faraday discovered electromagnetic induction effect and then produced a steady electric current. The following extensive and in-depth study of electricity was not only the main driving force of the second industrial revolution but also the foundation of the third revolution of science and technology. Until now, our daily life and industrial production cannot be separated from electric energy.

Alternating current and direct current

Electricity is the basic physical phenomenon associated with static or moving electric charges. The directional motion of electric charges forms the electric current. The electric current whose magnitude and direction changes with time is called alternating current (AC), and that whose direction does not change with time is called direct current (DC). Furthermore, the current whose both magnitude and direction do not change with time is called constant direct current or in short constant current. With different characteristics, AC and DC play their respective roles in every aspect of our lives and build the foundation of modern power electronics and technology. In recent years, AC has been widely applied in power transmission owing to its high efficiency, ease of boosting and decreasing voltage, and simple and convenient production equipment. As for DC, it is preferable for powering the widely distributed electronics, electrolysis, and electroplate. With the development of ultra-high-voltage transmission technology of DC (Huang et al., 2009), we need to re-examine the significance and applications of DC in new horizon.

Energy demand of electronics: constant current

A notable technological trend of our society is the exponential growth of mobile electronic devices and sensor networks, which are marching into every corner of our lives and greatly improving the quality of

[1]Beijing Institute of Nanoenergy and Nanosystems, Chinese Academy of Sciences, Beijing 100083, P. R. China

[2]College of Nanoscience and Technology, University of Chinese Academy of Sciences, Beijing 100049, P. R. China

[3]School of Materials Science and Engineering, Georgia Institute of Technology, Atlanta, GA 30332, USA

[4]These authors contributed equally

*Correspondence: zhong.wang@mse.gatech.edu (Z.L.W.), wangjie@binn.cas.cn (J.W.)

https://doi.org/10.1016/j.isci.2020.102018

our life. Generally, the energy demand of most electronic devices is a constant current input to realize sustainable working. The state of the art of energy sources for powering those electronics is mainly limited to batteries. However, batteries have limited life time that needs to be constantly monitored, need to be timely charged or replaced, and require huge manpower and material resources costs as well as bring environmental pollution problem (Larcher and Tarascon, 2015).

The invention of TENG

As the world is entering the era of internet of things (IoTs), sensor networks, big data, robotics, and artificial intelligence, its sensors are mobile and ubiquitous, and its electronic devices are following a general trend of miniaturization, portability, and functionality (Wang, 2019). Based on TE effect and electrostatic induction, triboelectric nanogenerator (TENG) was first invented by Wang's Group in 2012 (Fan et al., 2012), and it has attracted significant attention as an emerging mechanical energy harvesting technology owing to its various merits of simple structure, light weight, diverse choice of materials, low cost, and high efficiency even at low frequency (He et al., 2020; Lin et al., 2013; Luo et al., 2019; Peng et al., 2019, 2020; Song et al., 2019; Xiong et al., 2020; Yang et al., 2019; Zhang et al., 2018a, 2018b; Zhu et al., 2014b). Generally, the output of TENG is AC pulse feature, which must be converted to a DC output or even a constant current output across the power management circuit for powering electronics (Harmon et al., 2020; Niu et al., 2015; Qin et al., 2018; Xi et al., 2017; Xu et al., 2019b; Zhang et al., 2020b). Recently, some studies about TENGs with DC output are emerging, which are named as DC-TENGs (Liu et al., 2019a, 2020a; Luo et al., 2018; Xu et al., 2020a; Yang et al., 2014; Zhang et al., 2014; Zhu et al., 2020). Compared with AC-TENG, DC-TENG has unique merits of direct current characteristics to drive electronics without any rectifier or even energy storage unit, and thus shows great potential for practical applications. Up to now, strategies such as rotary rectifier bridge (Kim et al., 2018; Qiao et al., 2021; Zhang et al., 2014), double-wheel design (Yang et al., 2014), multiphase rotation-type structure (Kim et al., 2018; Li et al., 2020c; Qiao et al., 2021; Ryu et al., 2018; Wang et al., 2020b), contact-separation-type structure (Dharmasena et al., 2020), and electrostatic breakdown effect (Liu et al., 2019a; Luo et al., 2018; Yang et al., 2014) have been used for realizing DC output in TENG. Exploring the full potential of TENG from new structures and even new principle to realize DC output is highly desired for accelerating the miniaturization of IoTs and self-powered systems and may promote the understanding of TENG from a new horizon.

In recent years, there are several elaborate reviews about AC-TENG (Wang, 2014, 2020b; Wang and Wang, 2019; Wu et al., 2019; Zhou et al., 2020b). However, the studies of DC-TENG have not been reviewed till now. We believe a timely review on this topic is very important for future development of the new-generation TENG. In this review, some basic principles of AC-TENG are briefly summarized to have an insight on the physical fundamentals of DC-TENG; then DC-TENG arising from electrostatic induction and electrostatic breakdown is introduced, and the constant current output TENG with a series of optimization methods from various perspectives is also summarized. Furthermore, AC/DC-TENG is introduced to discuss the relationship of TE, electrostatic induction, and electrostatic breakdown. In addition, some new DC generators are also summarized for a wide range of readers, and the general TENG is proposed and defined as the generator that is based on contact electrification (CE) effect in nanoscale as shown in Figure 1 (the special TENG is based on CE and electrostatic induction). Finally, the major challenges and the future perspectives in this rapidly emerging research field are discussed.

FUNDAMENTAL PHYSICS OF TRIBOELECTRIFICATION

TE is always regarded as a negative effect, so it is only applied in a limited number of fields (Pingali et al., 2009; Pu et al., 2009; Salama et al., 2013; Sayfidinov et al., 2018). Until the invention of TENG in 2012 by professor Wang's group, this situation has dramatically changed (Fan et al., 2012). Recently, Wang et al. pointed out that CE is referred to as the scientific term of TE, which means that TE is not only related to the charge transfer due to physical contact but also to the tribology involved in the mechanical contact/sliding of two materials (Wang, 2020b; Wang and Wang, 2019).

Although CE has been documented from 2,600 years ago, its scientific understanding remains inconclusive, unclear, and un-unified (Shaw, 1926). After centuries of research, it is still not clear whether electrons, ions, or even bulk material transfer is responsible for the observed charging. Very recently, by using the Kelvin probe force microscopy (KPFM) to study the fundamental mechanism of CE, a conclusion that electron transfer is the dominant mechanism of CE between metal-polymer pairs is obtained (Li et al., 2016; Wang and Wang, 2019). As for liquid-solid cases, it is revealed that there are both electron transfer and

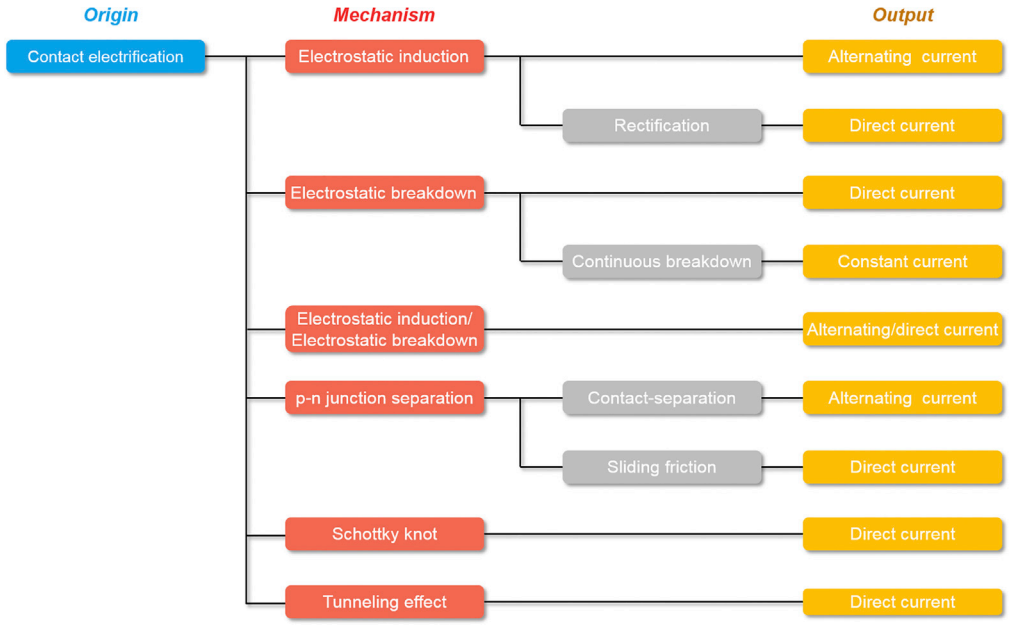

Figure 1. The mechanism and outputs of generalized TENG based on CE

ion transfer, where electron transfer plays a dominant role in liquid-solid CE (Lin et al., 2020b; Wang, 2020b).

The distance between two atoms where CE occurs is explored by measuring the surface potential using KPFM in a tapping mode (Li et al., 2016; Lin et al., 2020a). The surface potential difference between the center of scanned region and the edge after the second KPFM scan is presented in Figure 2. By adjusting the free vibration amplitude of the tip, they found that the distance of two atoms for electron transfer should be smaller than the interatomic distance at equilibrium, which means that CE is a process of nanoscale charge transfer. Generally, the role played by mechanical force is to make the two materials contact with each other and to shorten the distance between two atoms, and then cause a strong overlap of their electron clouds. The detailed description can be found in a recent review (Wang and Wang, 2019).

AC-TENG

Working modes of AC-TENG

Based on TE effect and electrostatic induction, the conventional TENG has two built-in characteristics, i.e., AC output consisting of pulsed series. Considering the direction of polarization change and the complex practical application scene, four basic working modes of the AC-TENG have been proposed to harvest all kinds of energy (Wang, 2014), which are vertical contact-separation mode, sliding mode, single-electrode mode, and freestanding triboelectric-layer mode, as shown in Figure 3.

The vertical contact-separation mode TENG uses the vertical direction of polarization change to induce electron flow in two electrodes, as shown in Figure 3A. This mode has the advantage of long working life easily up to 1,000,000 cycles due to the little surface abrasion and has been widely used in mechanical energy harvesting, self-powered sensor, implantable medicine, wearable electronics, and blue energy (An et al., 2019; Fan et al., 2012; Guo et al., 2018; Ouyang et al., 2019; Pu et al., 2017b; Wang et al., 2020a; Yin et al., 2019; Zhu et al., 2012). The lateral-sliding mode TENG is the same as the vertical contact-separation mode in structure, but the mechanical force applied on the charged surface is parallel to the contact surface (Figure 3B), which has been applied in sensitive nano-coulomb molecular mass spectrometry (Li et al., 2017) as well as microfluidic transport system (Nie et al., 2018), etc. The above-mentioned two working modes have two electrically connected electrodes, but in some cases, a part of AC-TENG is a free object without having an attached electric connection. To harvest this part of mechanical energy, single-electrode mode has been invented (Figure 3C). This mode has significant merits for energy harvesting in some special

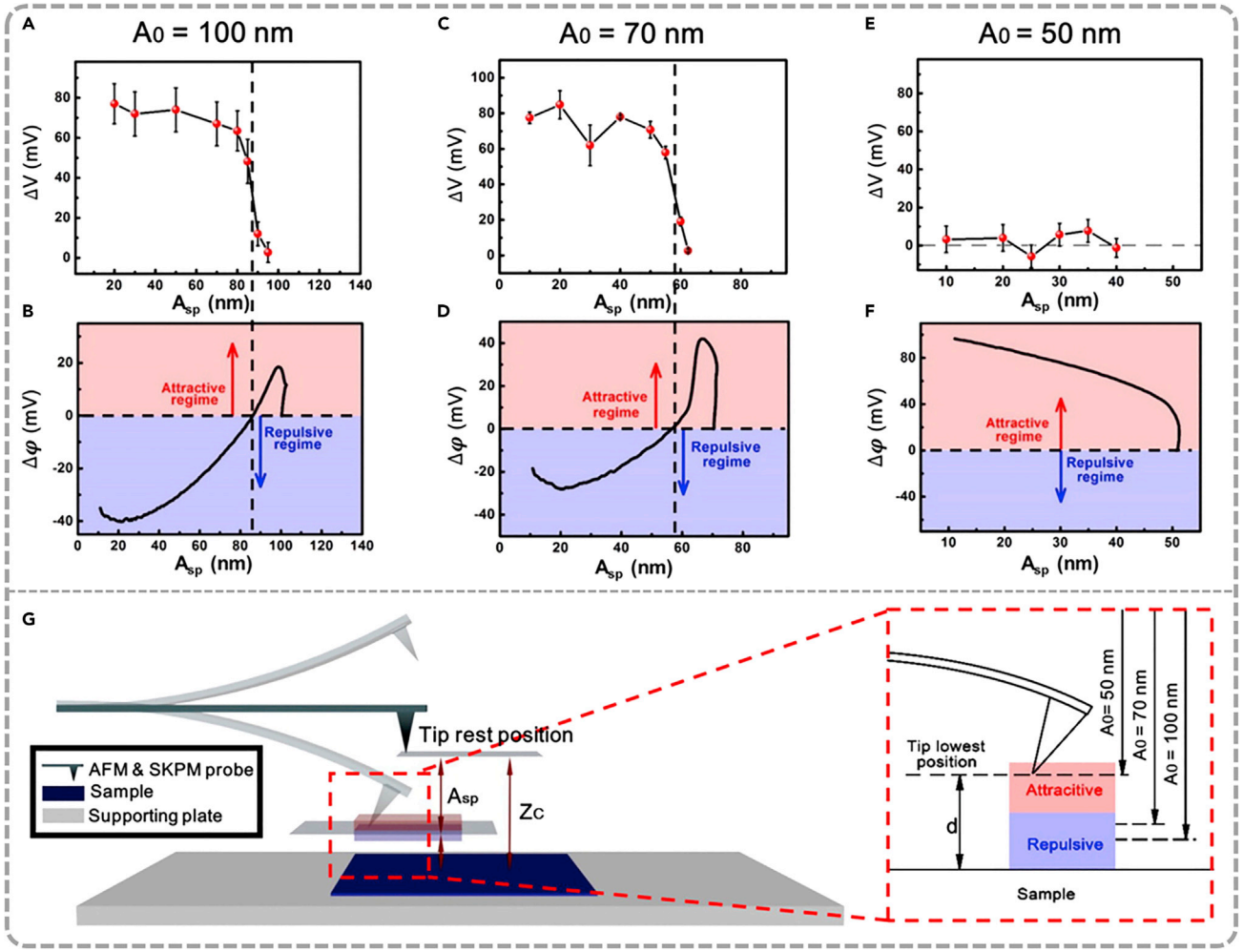

Figure 2. The relationship of CE and the change of phase shift ($\Delta\phi$) during the tapping vibration to probe the force zone within which charge transfer occurs

Adopted from (Li et al., 2016).

(A–F) The relationship of ΔV-A_{sp} and $\Delta\phi$-A_{sp} with A_0 = 100 nm, 70 nm, and 50 nm.

(G) The schematic diagram of the tip-sample interaction force of trapping scans with different scanning parameters (A_0 and A_{sp}).

cases such as human working, finger typing, motion sensor, raindrop, and more (Lin et al., 2014; Ma et al., 2020; Niu et al., 2014; Pu et al., 2017a; Wu et al., 2018; Yang et al., 2013). The freestanding triboelectric-layer mode is also invented for harvesting mechanical energy from the free object (Figure 3D). This mode is suitable for harvesting mechanical energy through rotational motions like airflow and water flow, which has been widely used for electrochemistry, energy storage, environmental mechanical energy harvesting, angle sensor, and high-voltage power sources (Cheng et al., 2018a; Han et al., 2020; Wang et al., 2014b, 2020c; Zhou et al., 2019; Zhu et al., 2014a).

From the point of view of moving direction and the capacitance change, four basic working modes can be divided into two types: contact-separation-type and sliding-type AC-TENG, both of which are considered as an electric charge source combining a capacitor with varying capacitance using the capacitor model (Figure 3E) (Niu and Wang, 2015; Wu et al., 2019). With repeated change in the distance between the two planes (corresponding to the contact-separation-type AC-TENG) and the size of contacting area (corresponding to the sliding-type AC-TENG) by external force, the capacitance between the two electrodes in AC-TENG varies and results in electrons flowing back and forth in external circuit to balance the potential difference between the two electrodes, generating an AC output. Compared with the contact-separation-type AC-TENG, the sliding-type AC-TENG can be simply made into rotation structure, which has been

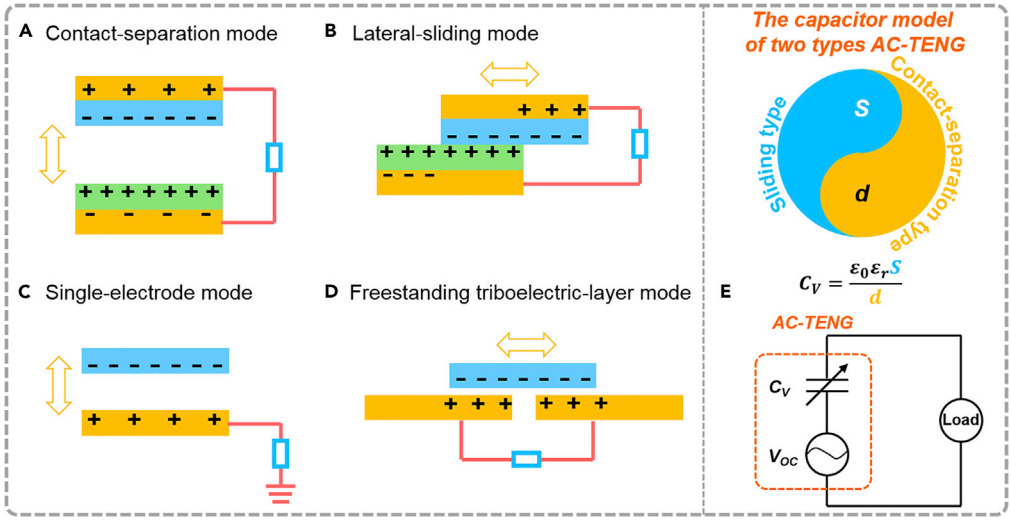

Figure 3. Four working modes of AC-TENG

(A–D) (A) The contact-separation mode, (B) lateral-sliding mode, (C) single-electrode mode, and (D) freestanding triboelectric-layer mode TENG.

(E) The capacitor model of two types of AC-TENG.

widely used in rotary mode energy harvesting such as wind and water flow energy. The sliding-type AC-TENG has the advantage of high efficiency of TE but the disadvantage of low durability due to surface abrasion (Zhou et al., 2016). Recently, the durability of sliding-type AC-TENG was significantly enhanced by automatic transition between contact and noncontact working states (Chen et al., 2020b; Li et al., 2015).

Maxwell's current

With deep research in the field of TENG, the fundamental physics mechanism of TENG is considered as it uses displacement current as the driving force for effectively converting mechanical energy into electric energy (Wang, 2017, 2020a), and the displacement current density is defined as

$$J_D = \frac{\partial D}{\partial t} = \varepsilon \frac{\partial E}{\partial t} + \frac{\partial P_S}{\partial t} \quad \text{(Equation 1)}$$

where the total displacement current density is J_D, the electric displacement vector is $\boldsymbol{D}$, the medium polarization vector is $\boldsymbol{P}_S$ (here, $\boldsymbol{P}_S$is mainly due to the existence of surface charges that are independent of the presence of electric field), and the electric field is $\boldsymbol{E}$. By integrating the displacement current density at the surface, the displacement current (I_D) can be obtained, as follows:

$$I_D = \int J_D dS = \int \frac{\partial D}{\partial t} dS = \frac{\partial}{\partial t} \int \nabla \cdot D dr = \frac{\partial}{\partial t} \int \rho dr = \frac{\partial Q}{\partial t} \quad \text{(Equation 2)}$$

where the medium surface is $\boldsymbol{S}$, the field point is $\boldsymbol{r}$, the distribution of free charges is ρ, the total free charge on the electrode is Q. As we mentioned above, AC-TENG can be referred to as capacitive conduction, also named capacitive model. From Equation (2), we can find that the capacitive conduction current in external circuit is equivalent to the displacement current in internal circuit, and they form a complete loop in two electrodes (Figure 4). In other words, the displacement current in internal circuit is the physical core driving force for power generation, and the observed conduction current in external circuit is the external manifestation of displacement current. For AC-TENG, the output current in external circuit is driven by the displacement current inside the generator, which physically represents an alternating electric field caused by periodic external mechanical force that uses displacement current as the driving force to drive electron flow in electric wire. From the perspective of the fundamental driving force, an alternating electric field will cause an AC output in external circuit. From the aspect of the structure of the AC-TENG, electrons cannot across the dielectric layer to transport, and electrons will alternatively transfer between the two electrodes because of the periodically changed potential difference in two electrodes (for single-electrode mode TENG, the grounded is considered as the other electrode), and then an AC output can be obtained in external circuit. This is the basic mechanism of why the conventional TENGs have an AC output.

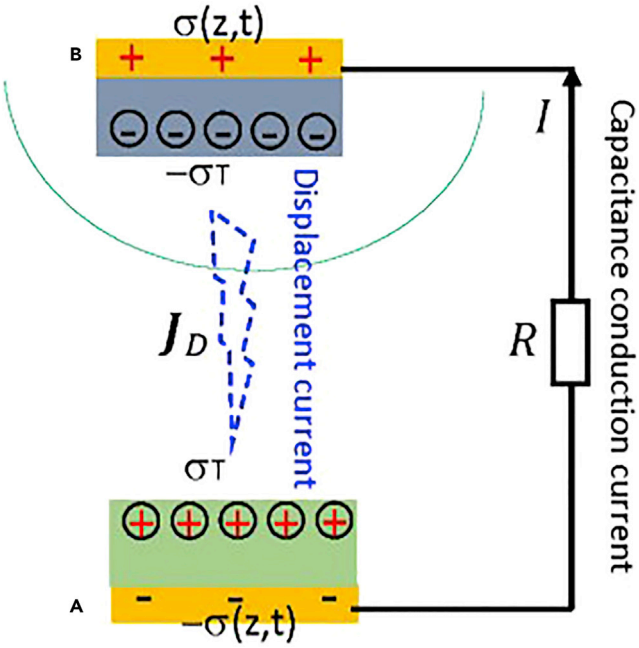

Figure 4. Working mechanism of TENG with contact-separation mode
Adopted from (Wang, 2020a)

Figure of merits of TENG

To evaluate the output performance of different working modes from the perspective of material, structure, and whole performance, and even to compare with other energy harvesting technologies, a specialized figure of merit (FOM) for defining the performance of an AC-TENG was reported by Zi et al. (2015). Taking the lateral-sliding mode AC-TENG as example, the continuous periodic sliding motion can generate a time-dependent periodic electrical output signal, and the schematic diagram of the lateral-sliding mode AC-TENG with the displacement defined is shown in Figure 5A. A switch in parallel with the external load is used to realize instantaneous short-circuit conditions when the relative displacement is $x = 0$ and $x = x_{max}$ (Figure 5B). In such cases, the area of *V*-*Q* plot increases with the load resistance, and then up to the maximum with infinite external load, which is the open-circuit condition. Similarly, we can find that the output energy of all four working modes is limited inside the area of the trapezoid.

Based on those definitions, the $FOM_{S,max}$ of different working mode TENGs has the following relationship: CFT > CS > SFT > LS > SEC, where CFT is the contact freestanding triboelectric-layer structure, CS is the vertical contact-separation structure, SFT is the sliding freestanding triboelectric-layer structure, LS is the lateral sliding structure, and SEC is the single-electrode contact structure, as shown in Figure 5C. In addition, they defined a normalized triboelectric charge density and a dimensionless FOM_M, where the triboelectric performance between fluorinated ethylene propylene and the liquid metal is the reference (Figures 5D and 5E). Given that the conventional triboelectric series is the qualitative description of the performance of CE between two different materials, the quantitative measurement of the transferred charges between two materials is more important and useful for designing high-performance AC-TENG (Zou et al., 2019, 2020). Furthermore, the FOM_M is still suitable for the DC-TENG, which will be discussed in the following section.

Electrostatic breakdown in TENG

Like TE effect, electrostatic breakdown is also a common natural phenomenon and lightning is caused by TE effect and electrostatic breakdown in air. Due to the existence of electrostatic breakdown in TENG, the limitation factors of surface charge density of AC-TENG ($\sigma_{AC\text{-}TENG}$) can be described as (Wang et al., 2017):

$$\sigma_{AC\text{-}TENG} = \min(\sigma_{triboelectrification}, \sigma_{r,\ air\ breakdown}, \sigma_{dielectric\ breakdown}) \quad \text{(Equation 3)}$$

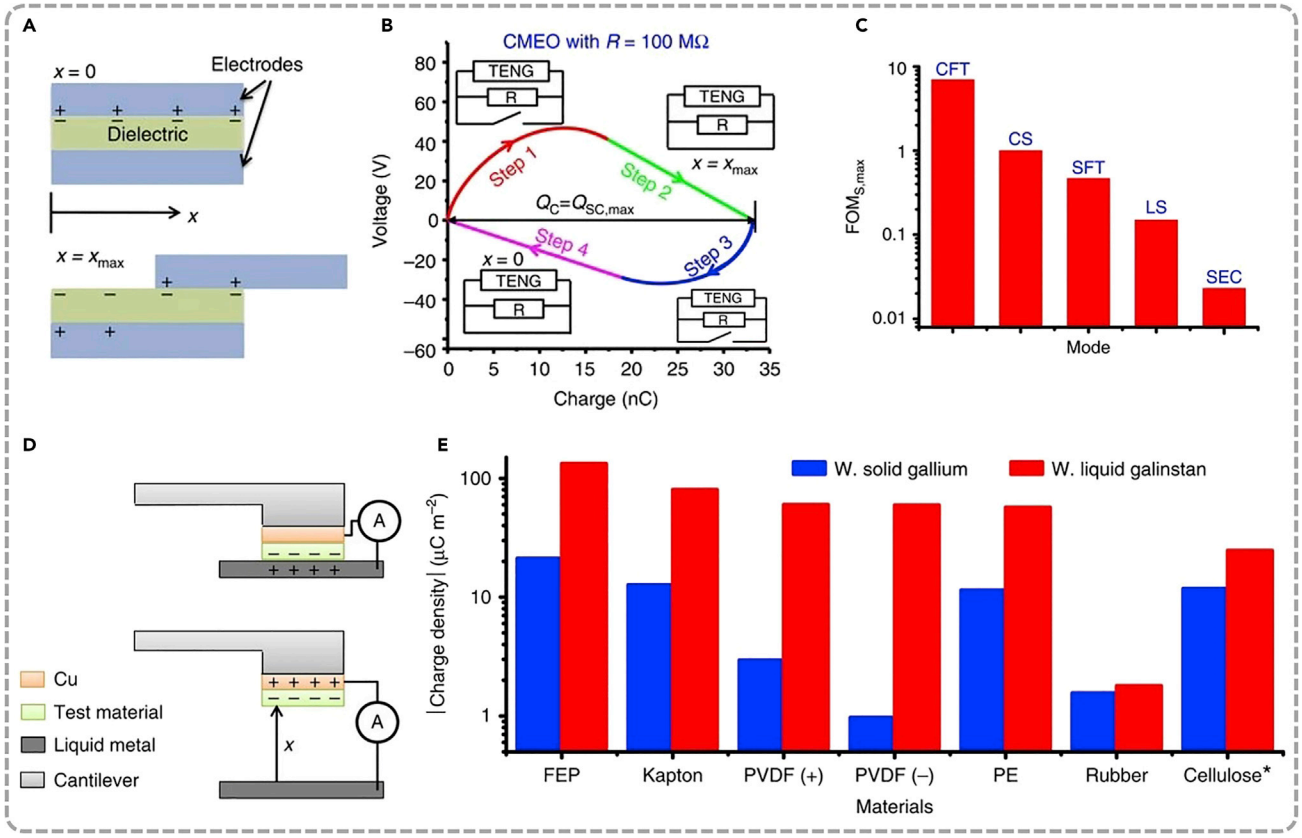

Figure 5. Figure of merits for TENGs

Reprinted from (Zi et al., 2015) with permission, Copyright©2015 Springer Nature.

(A) Schematic diagram of the LS mode TENG.

(B) The cycles for energy output at the load resistance of 100 MΩ.

(C) The maximum FOM_s of different structural TENG from FEM simulations.

(D) The measurement diagram with liquid metal as one electrode.

(E) The charge density of various materials with solid gallium and liquid galinstan.

where $\sigma_{triboelectrification}$ represents the TE charge density, $\sigma_{r,\ air\ breakdown}$ is the remaining charge density after air breakdown, and $\sigma_{dielectric\ breakdown}$ represents the maximum charge density that the dielectric layer can store. The output performance of AC-TENG can be increased with the improvement of $\sigma_{triboelectrification}$ by materials optimization (Zou et al., 2019, 2020) and structural design (Chun et al., 2016; Wang et al., 2016a), whereas breakdown effect gradually becomes a bottleneck problem for all modes of AC-TENGs that must to be considered, resulting in the limitation of $\sigma_{r,\ air\ breakdown}$ (Wang et al., 2014a, 2017; Zhang et al., 2020a; Zi et al., 2017). Then, high-vacuum environment was used to avoid air breakdown (Wang et al., 2017); the ultra-thin triboelectric layer was used to reduce the electrostatic field across two triboelectric layers and finally elevate the threshold of $\sigma_{r,\ air\ breakdown}$, consequently obtaining a high triboelectric charge density (Zhang et al., 2020a). Furthermore, the external charge excitation method is used to avoid the air breakdown in the main TENG, in which charges are stored in two electrodes rather than on the surfaces of two triboelectric layers (Cheng et al., 2018b; Liu et al., 2019c, 2020c; Wang et al., 2020a; Xu et al., 2018). In a word, the output performance of AC-TENG can be greatly improved by avoiding the breakdown effect. Alternatively, a new type of TENG by using breakdown effect is also a complementary method for further enhancing the output performance of TENG as a directly robust power source with their unique characteristics (Liu et al., 2019a, 2020b; Zhou et al., 2020a), and this part will be discussed in the following section.

DC-TENG

Based on TE and electrostatic induction, the conventional TENG (AC-TENG) has the distinct characteristics of AC with pulsed series, and the output current usually also has high crest factor (Ryu et al., 2018). Given

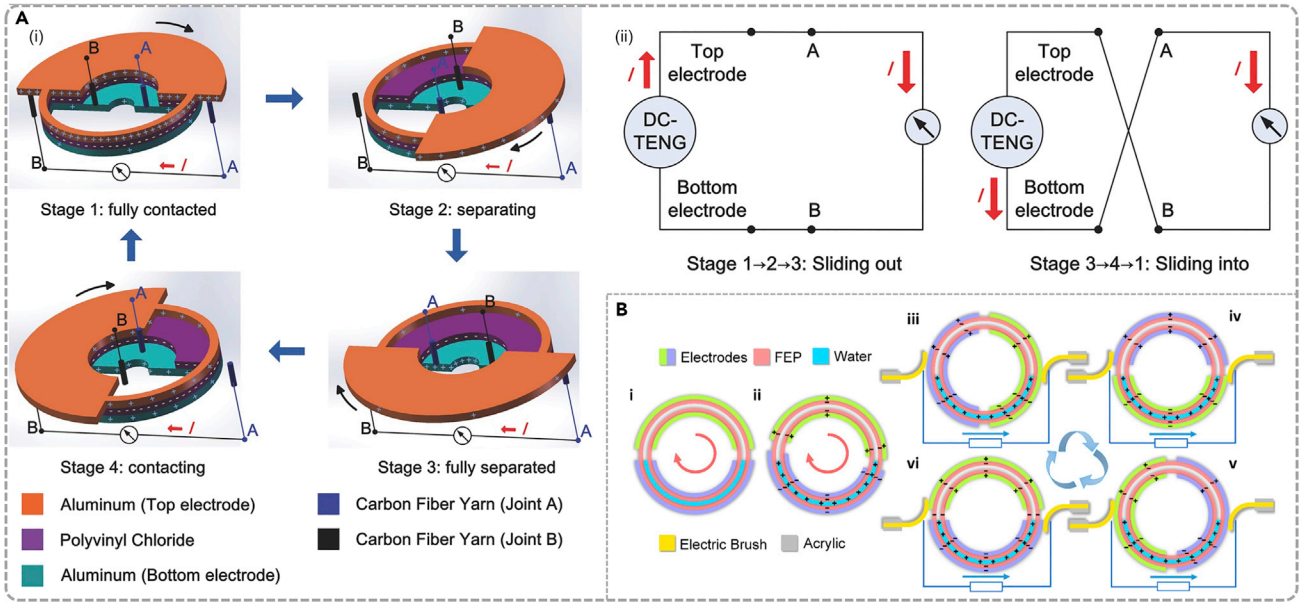

Figure 6. Mechanical rectifier for TENG

(A) (i) Schematic diagram of a rotating disk design for converting rotational mechanical energy to electric energy and its working mechanism. (ii) Equivalent circuit diagrams of the rotating disk-based DC-TENG in different stages. Adopted from (Zhang et al., 2014).

(B) The schematic diagram and working mechanism of the DC-TENG based on liquid dielectrics. Adopted from (Wang et al., 2019).

that most electronics work at a constant current condition, the development of DC output or even constant current output power source has obvious advantages for the miniaturization of self-powered systems and the high efficiency of energy storage (Li et al., 2020b; Liu et al., 2019a, 2020b; Zhou et al., 2020a). Some methods have been reported to realize DC output arising from electrostatic induction, such as mechanical rectifier and phase control (Kim et al., 2018; Li et al., 2020c; Qiao et al., 2021; Ryu et al., 2018; Wang et al., 2020b; Zhang et al., 2014). Furthermore, breakdown effect is innovatively used for restricting the direction of electron transfer and shows particularly characteristics of simple structure and high energy conversion efficiency (Liu et al., 2019a).

DC-TENG arising from electrostatic induction

Mechanical rectifier

Conventional TENG from electrostatic induction has the intrinsic characteristics of AC output due to the alternatively flowing of induced electrons between two electrodes by the electrostatic field. Based on this working mechanism, some innovative strategies have been reported to obtain DC output by duly exchanging the position of two electrodes in the equivalent circuit, in which the "exchanging manner" realized by mechanical structure is similar to the rectifier in electronic components. Zhang et al., 2014 reported a DC-TENG based on a rotating disk design for converting rotational mechanical energy to electric energy, and its working mechanism is shown in Figure 6A(i). Due to the opposite direction of output current in conventional sliding mode TENG, the reversible joints will cause a DC output in the whole cycle, as shown in Figure 6A(ii). Wang et al. (2019) reported a multifunctional DC-TENG based on liquid dielectrics interface, and the two electric brushes are rationally designed to contact the two electrodes, respectively. The working mechanism of the liquid dielectrics DC-TENG is shown in Figure 6B. Because the two electrodes alternatively contact the electric brush, the direction of the output current will not change. Very recently, Qiao et al. (2021) reported a new design in which the AC output of a rotatory-sliding TENG is converted into DC output with the assistance of the mechanical rectifier, which consists of the rolling electric brushes and the commutator.

Phase control

To further decrease the crest factor of TENG's output and even obtain the constant current output, which is often necessary for directly powering electronic devices, some studies reported a method by phase control for converting mechanical energy into DC with low crest factor. Ryu et al. (2018) reported multi-phase

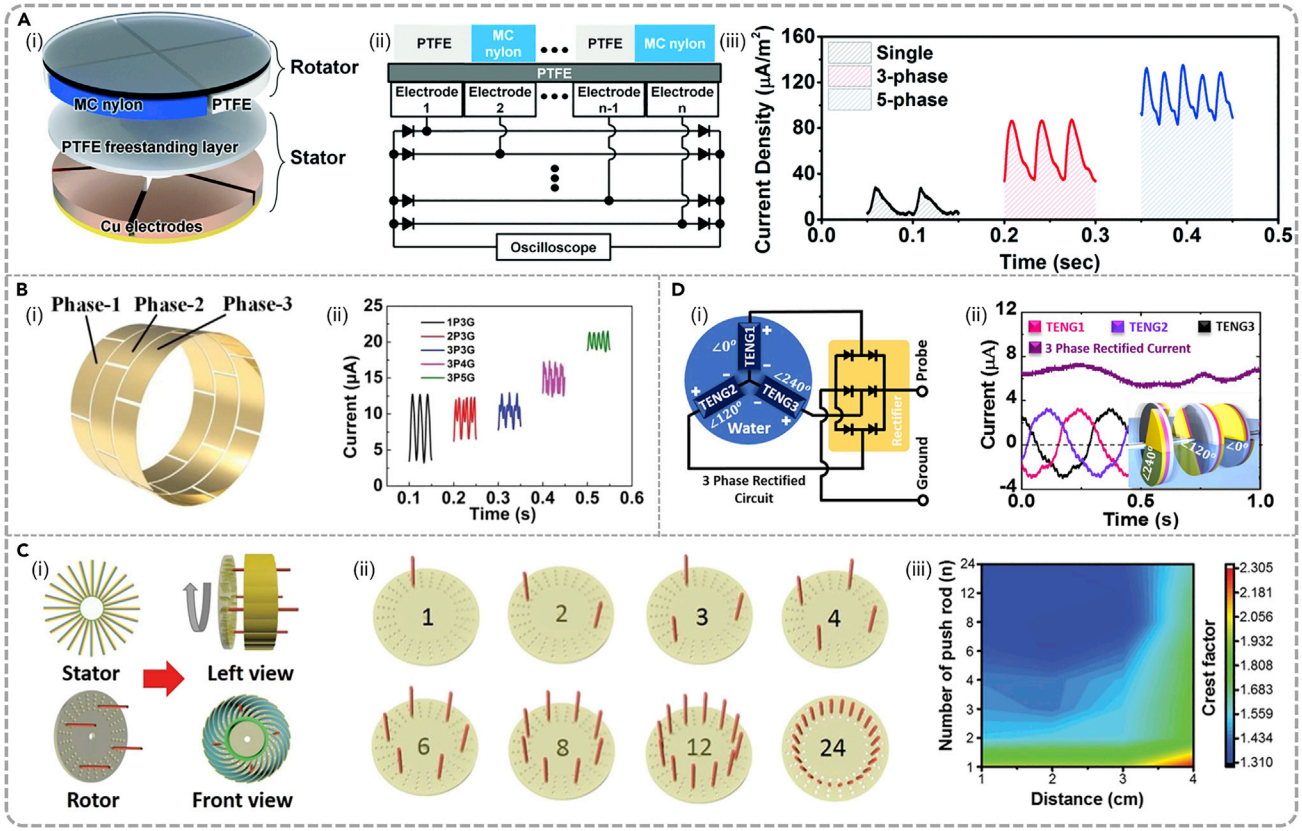

Figure 7. Phase control for TENG

(A) (i) Schematic description of the multi-phase rotation-type TENG. (ii) Multi-phase management circuit diagram of the MP-TENG. (iii) Output voltage of the MP-TENG with different phases during one cycle. Adopted from (Ryu et al., 2018).

(B) (i) Schematic diagram of the structural relationship of phase and group in this DC-TENG. (ii) Output current of the DC-TENG with unanimous phases and different groups. Adopted from (Wang et al., 2020b).

(C) (i) Schematic description of M-TENG and its detailed structure. (ii) The distribution of push rods in MRM-TENG. (iii) The relationship of output current crest factor, number of push rods, and the distance. Adopted from (Li et al., 2020c).

(D) (i) Schematic diagram showing the experimental method for fabricating this DC-TENG with three disks and a three-phase rectifier circuit. (ii) The curves of three-phase rectified current and respective current. Adopted from (Kim et al., 2018).

rotation-type TENGs (MP-TENGs) as shown in Figure 7A(i). Here, the AC output in each electrode is rectified by using the full-wave bridge rectifier, which is shown in Figure 7A(ii). Each pair of polytetrafluoroethylene (PTFE) and nylon layer has a regularly different contact ratio to regularly shift the current phases. With an increase in the number of phases, both the peak values and minimum values of output current density are significantly increased, but the current crest factor reduced from 2.01 to 1.26 for 5-phase TENG (Figure 7A(iii)). Wang et al. (2020b) fabricated a cylindrical DC-TENG that can generate an almost constant current output with low crest factor, which mainly contains a rotator and a cylindrical stator. This DC-TENG is divided into different groups (G) and phases (P) as shown in Figure 7B(i). By changing the number of groups and phases, the output current can be greatly increased, whereas the crest factor decreased (Figure 7B(ii)), and the DC-TENG with 3P5G shows the greatest output performance. Li et al. (2020c) reported a rotational contact-separation mode TENG with multiple electrodes to largely enhance the durability of rotation mode TENG (Figure 7C(i)). More importantly, the crest factor of output current can be decreased to a relatively low value by adjusting the phase difference and device numbers (Figures 7C(ii) and 7C(iii)). To further address the durability issue of DC-TENG, Kim et al. (2018) proposed a water electrification mode TENG that can generate DC output based on phase control to enhance the sustainability of TENG. They fabricated three disks of TENGs with a 120° phase difference among this three TENGs, and the three-phase rectified circuit is shown in Figure 7D(i). The output current of this mode can be reinforced after integrating with each other (Figure 7D(ii)), and its output performance can be further elaborated by increasing the number of disks and controlling the phase differences.

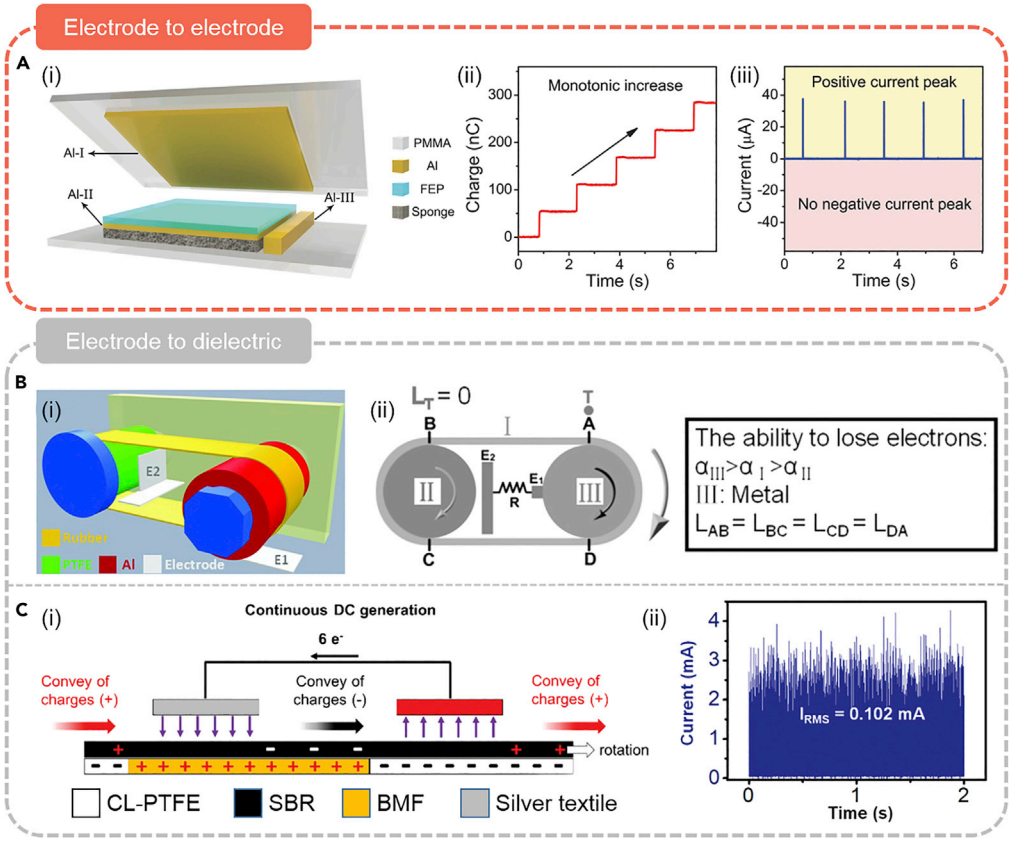

Figure 8. DC-TENG arising from dielectric breakdown

(A) (i) The structure of the DC-TENG by utilizing the air breakdown-induced ionized air channel. (ii) Transferred charges and (iii) short-circuit current of the DC-TENG. Adopted from (Luo et al., 2018).

(B) (i) The schematic diagram of the DC-TENG. (ii) The working mechanism and the ability to lose electrons in this DC-TENG. Adopted from (Yang et al., 2014).

(C) (i) The overall working mechanism for the continuous DC generation. (ii) The output current of this microdischarge-based DC-TENG. Reprinted from (Yoon et al., 2020) with permission, Copyright©2020 Wiley-VCH Verlag GmbH & Co. KGgA, Weinheim.

DC-TENG arising from dielectric breakdown

Besides the aforementioned methods for realizing DC output from electrostatic induction, the strategy arising from dielectric breakdown shows particularly characteristics of simple structure and high energy conversion efficiency to produce the DC output. The breakdown process limits the flowing of electrons in the single direction, making the electric components such as rectifier unnecessary.

The breakdown phenomenon can be divided into two types: electrode to electrode and electrode to dielectric. Luo et al. (2018) reported a DC-TENG to harvest the contact-separation mechanical energy by utilizing the air breakdown-induced ionized air channel between two electrodes. Figure 8A(i) is the basic structure of this DC-TENG. Figure 8A(ii) shows a monotonic increase trend of the output charge, and there is only positive current peak in Figure 8A(iii) without negative current peak, which both indicate the good DC output characteristics. This working mechanism was also verified by photocurrent signal detection and controllable discharging observation, providing some methods for detecting the air breakdown phenomenon.

The other breakdown phenomenon occurs between the electrode and dielectric. Yang et al. (2014) reported a DC-TENG based on sliding electrification for harvesting rotary mechanical energy. This DC-TENG comprises two wheels and one belt as shown in Figure 8B(i). The most important condition in this DC-TENG is that the ability to lose electrons should satisfy the relationship: III > II > I (Figure 8B(ii)).

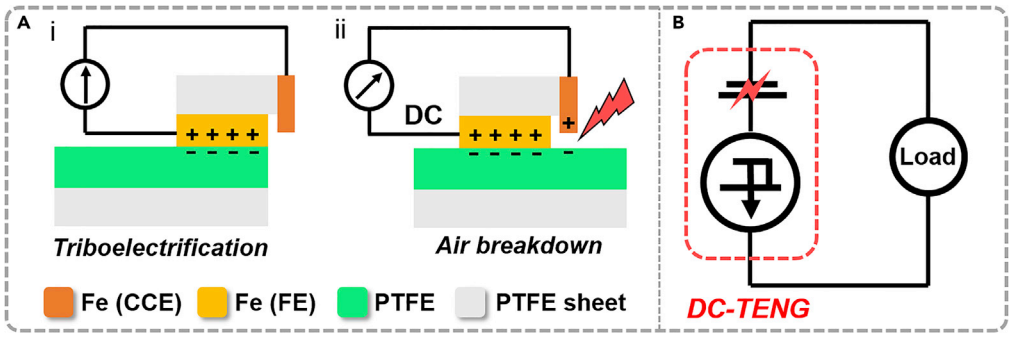

Figure 9. Constant current TENG arising from electrostatic breakdown

Adopted from (Liu et al., 2020b).

(A) Working mechanism of the sliding mode DC-TENG.

(B) The basic principle of the DC-TENG from a circuit perspective.

Recently, Yoon et al. (2020) reported a micro-discharge-based DC-TENG via accumulation of triboelectric charges in atmospheric condition (Figure 8C(i)). Figure 8C(ii) is the DC output of this DC-TENG with the half-disk pair at 500 r min^{-1}, and the root-mean-square current is up to 0.102 mA.

The constant current TENG arising from electrostatic breakdown

As for most electronic devices, a power supply with the constant current output is always needed for sustainable and continuous working. Given that the output charge density of TENG in air is lower than the value in vacuum. Taking a 50-μm PTFE triboelectric layer as an example, the theoretical charge density of around 250 μC m^{-2} is much lower than the achieved value of around 1,000 μC m^{-2} in vacuum, where a dominant part is wasted by air breakdown (Wang et al., 2017). Liu et al. (2019a) innovatively designed a structure to harvest the breakdown energy. This novel DC-TENG, arising from electrostatic breakdown, can produce a constant current output, which has been demonstrated to directly power electronic devices without any rectifier and energy storage unit. The DC-TENG not only can promote the miniaturization of self-powered systems used in wearable electronics and sensor networks in IoTs but also can provide a paradigm-shifting technique for TENG to effectively convert mechanical energy into electric energy. Furthermore, it can be further considered as a prototype of lighting energy harvesting. In addition, it has been demonstrated for mechanical energy harvesting combining with the conventional AC-TENG to enhance the final energy output and self-powered sensor for measuring various motion parameters, showing great potential for application in energy and sensing (Yin et al., 2020; Zhou et al., 2020a).

Basic principle

The basic model of this DC-TENG is illustrated in Figure 9A. Its working mechanism is based on TE and electrostatic breakdown. When the frictional electrode (FE) contacts with the triboelectric layer (material: PTFE), electrons will transfer between two materials due to the different ability of losing electrons. As the PTFE is an electret, it can hold a quasi-permanent electric charge. When the slider moves on the dielectric layer and the charge-collecting electrode (CCE) reaches above the surface of the negative charged PTFE, a high electric field will build in the gap between the CCE and the PTFE layer. If the electrostatic field exceeds the dielectric strength of the atmosphere between them, air will be ionized and become conductive. Then, electrons will transfer from the surface of PTFE to the CCE and then to the FE in external circuit forming an electric loop. Thus, a continuous DC output can be obtained if a continuous external force applies on the slider.

Looking at the DC-TENG from a circuit perspective, it can be considered as an electric charge source and a broken-down capacitor in which the CCE/gap/PTFE serves as the capacitor, as shown in Figure 9B. The TE process can be considered as the charged process of PTFE surface. The CCE is rationally designed to induce a high voltage drop across the air gap, and the process of air breakdown is equivalent to a "switch" to timely release the voltage potential, and the "switch" is controlled by the avalanche breakdown process. It should be emphasized that the constant current output is strongly relied on whether the electric charge source can provide enough charges for air breakdown. Therefore, the

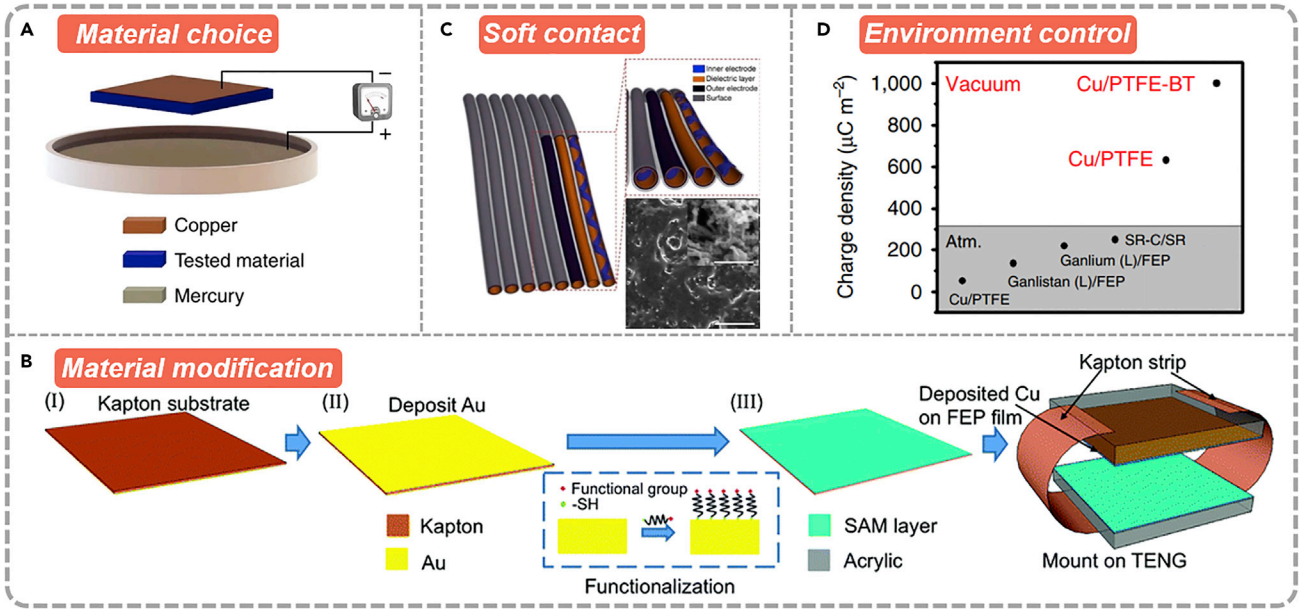

Figure 10. Enhancing the surface charge density

(A) The schematic diagram to quantitatively measure the triboelectric series over 50 polymers and nearly 30 inorganic nonmetallic materials with mercury as the other triboelectric layer. Adopted from (Zou et al., 2019).

(B) Material modification by chemical surface functionalization. Reprinted from (Wang et al., 2016b) with permission, Copyright©2016 Royal Society of Chemistry.

(C) Soft contact to improve contact intimacy. Adopted from (Wang et al., 2016a).

(D) Enhancing the surface charge density by environment control. Adopted from (Wang et al., 2017).

constant current TENG is built on sliding-mode TENG due to the high triboelectric efficiency in sliding mode (Zhou et al., 2016).

Optimization methods

The optimization methods of air breakdown DC-TENG can be briefly divided into two parts from its basic principle: improving the surface charge density, which is alike with the conventional AC-TENG, and enhancing the process of electrostatic breakdown.

The strategies for improving the surface charge density can be classified into three parts: material choice and modification, effective contact, and environmental control. It is very effective to choose a suitable pair of materials to enhance the triboelectric charge density and then improve TENG's output performance. Recently, Zou et al. (2019, 2020) quantified the triboelectric charge densities of over 50 polymers and nearly 30 inorganic nonmetallic materials with mercury as the other triboelectric layer, which may serve as a standard for materials choice of TENGs (Figure 10A). Surface modification is another method (Wang et al., 2016b) to increase the surface charge density (Figure 10B). In addition, by choosing elastomeric materials and a fragmental contact structure, the surface charge density can also be increased (Figure 10C) (Wang et al., 2016a). Furthermore, the environment condition also has a great effect on the surface charge density, such as the atmospheric pressure (Figure 10D) (Wang et al., 2017).

As for enhancing the process of electrostatic breakdown, it can be optimized by structural design and environmental control. The microstructure on the surface of triboelectric layer not only can increase the surface charge density but also can enhance the electric field around the microstructure to make it more prone for air breakdown. The CCE can also be rationally designed for enhancing the process of electrostatic breakdown. Furthermore, an appropriate gap distance is easier for gas breakdown. In addition, environmental conditions such as temperature and atmospheric pressure have great influence on the process of gas breakdown (Figures 11A–11D) (Liu et al., 2020b). At high vacuum where air breakdown is avoided, the output charge density of AC-TENG increases with the temperature increasing from 293 K to 473 K (Figure 11D). The output performance of a rotary DC-TENG also

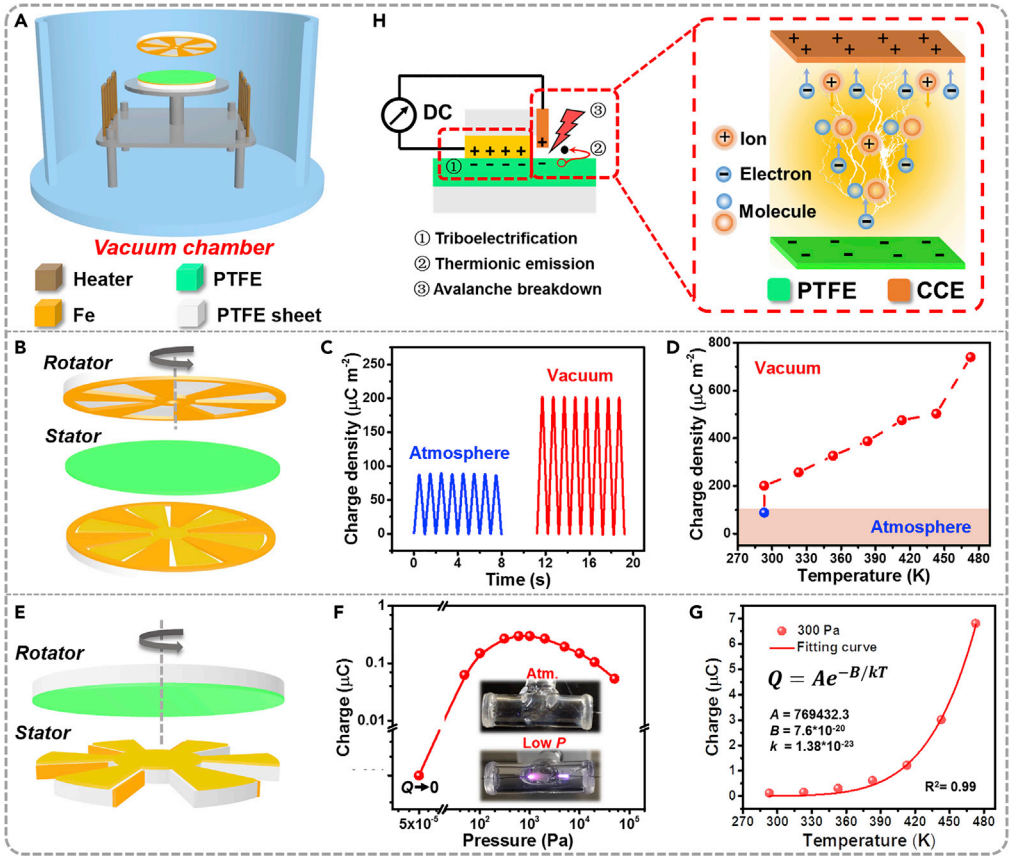

Figure 11. Enhancing the process of electrostatic breakdown

Adopted from (Liu et al., 2020b).

(A) A high-vacuum system with a heater to realize environment control.

(B–D) (B) The schematic diagram of the sliding mode AC-TENG. The output charge density of AC-TENG (C) in atmosphere and vacuum, and (D) at various temperatures under atmospheric pressure and high vacuum.

(E) The schematic diagram of the DC-TENG.

(F) Output charges in per cycle of the DC-TENG at various atmospheric pressures (insets show the breakdown phenomena in atmosphere pressure and low pressure).

(G) Transferred charges in per cycle at various temperatures with a pressure of 300 Pa. (H) The physical model of DC-TENG and the avalanche breakdown in DC-TENG.

confirmed the beneficial of low atmosphere pressure and high temperature for air breakdown (Figures 11E–11H).

Potential applications

This DC-TENG has been demonstrated to apply in energy harvesting and sensors (Liu et al., 2019a; Yin et al., 2020). Figure 12A(i) is the schematic diagram of the sliding mode DC-TENG. During the process of periodic sliding motion, it can produce good DC output, and an electronic watch can be directly powered without any rectifier and energy storage unit (Figures 12A(ii) and 12A(iii)). During the process of continuous rotary motion, a continuous and approximate constant current output was achieved as shown in Figures 12A(iv) and 12A(v). The constant current output can be directly power a light-emitting diode (LED) bulb array and these LEDs remain at constant luminance without flashing phenomenon (Figure 12A(vi)). Besides, a triboelectric vector sensor (TAS) based on this mode DC-TENG was reported by Yin et al. in a recent paper (Figure 12B(i)) (Yin et al., 2020). According to the experimental and theory analysis, they found that the TAS can realize probing multiple physical quantities in a self-powered manner, such as displacement, velocity, acceleration, angle, and angular velocity as shown in Figures 12B(ii)–12B(v). Given the aforementioned analysis, this DC-TENG shows great potential for mechanical energy harvesting in a wide range of atmosphere pressure and temperature, and for self-powered sensor including but not limited to motion monitoring and tracking.

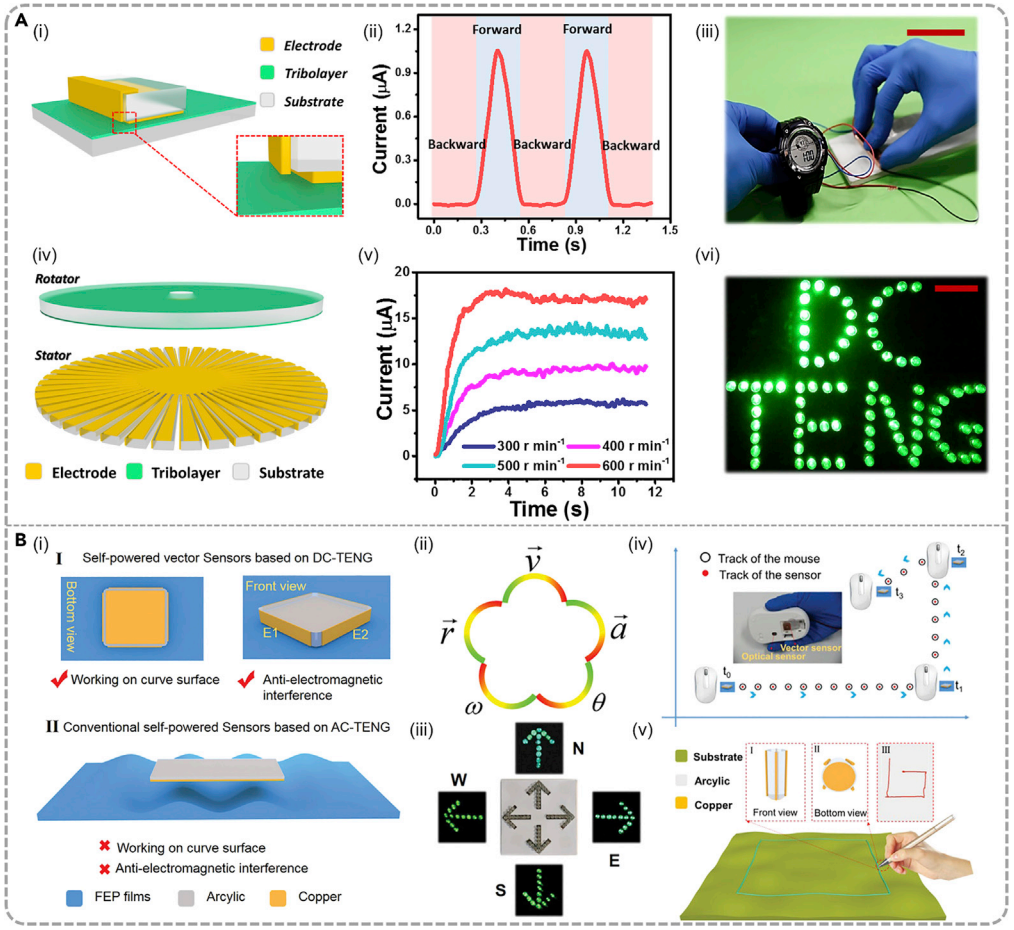

Figure 12. DC-TENG for energy harvesting and sensors

(A) (i) A schematic illustration of the sliding mode DC-TENG. (ii) The output current of the DC-TENG during the periodic sliding motion. (iii) The photograph of an electronic watch powered by a sliding mode DC-TENG. Scale bar = 5 cm. (iv) The schematic diagram of the rotary mode DC-TENG. (v) The output current of the rotary mode DC-TENG at various rotation speeds. (vi) The photograph of 81 LEDs with stable luminance directly powered by a rotary mode DC-TENG. Scale bar = 5 cm. Adopted from (Liu et al., 2019a).

(B) (i) The schematic structure of the self-powered motion vector sensor based on DC-TENG compared with the conventional self-powered sensors based on AC-TENG. (ii) Physical quantities obtained from the self-powered motion vector sensor. (iii) A self-powered directional sensor composed of the TVS system with some LEDs as indicator light. (iv) The tracks of the commercial mouse equipped with an optical sensor and the self-powered vector sensor. (v) The TVS works on the curved surface. Adopted from (Yin et al., 2020).

AC/DC-TENG

The relationship of triboelectrification, electrostatic induction, and electrostatic breakdown

TE effect is the basis of the new energy harvesting technology of AC-TENG arising from electrostatic induction and DC-TENG arising from electrostatic breakdown. From the point of view of charge utilization, the electrostatic charges created by TE are used for inducing charges flowing in external circuit by electrostatic induction or inducing ionization of gas to form a conductive path by electrostatic breakdown. It is thus natural to study the relationship of TE, electrostatic induction, and electrostatic breakdown. Generally, the charges created by TE in TENG can be used by electrostatic induction or electrostatic breakdown, namely, the charges from electrostatic induction plus the charges from electrostatic breakdown is the whole charge created by TE, as shown in Figure 13 (Zhou et al., 2020a). By rationally designing the structure of TENG and controling the working environment of TENG, the amount of output charges can be regulated by these two principles (electrostatic induction and electrostatic breakdown), which is similar to the Yin and Yang diagrams in traditional Chinese culture.

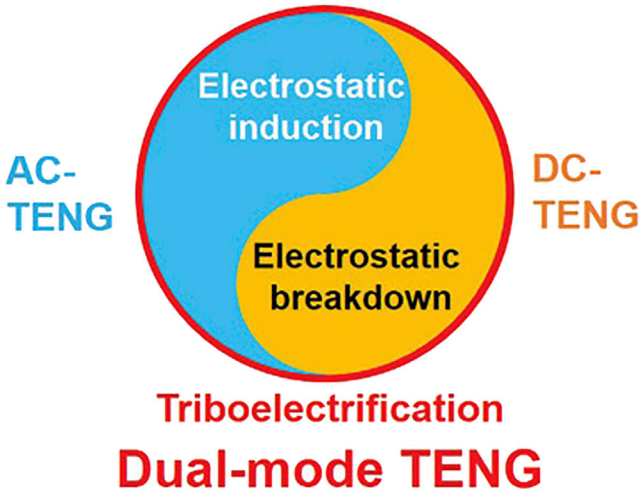

Figure 13. The relationship of triboelectrification, electrostatic induction, and electrostatic breakdown
Adopted from (Zhou et al., 2020a)

Design and applications of AC/DC-TENG

As the AC-TENG or DC-TENG can only harvest the electrostatic energy by electrostatic induction or breakdown separately, the invented AC/DC dual-mode TENG shows particular superiority in mechanical energy harvesting and self-powered systems compared with the single-mode TENG. The AC/DC dual-mode TENG is defined as the simultaneous harvesting of the electrostatic energy from CE by coupling of the two physical effects of electrostatic induction and electrostatic breakdown, which generally contains three types of electrodes in its structure: the FE, CCE, and induction electrode (IE). Zhou et al. (2020a) reported a novel AC/DC dual-mode TENG to simultaneously harvest mechanical energy by electrostatic induction and dielectric breakdown in a single device (Figure 14A(i)). Thanks to the coupling of the two principles, the whole energy output can be greatly enhanced. The working mechanism of the dual-mode TENG is shown in Figure 14A(ii). Figure 14A(iii) is the output charge density of the dual-mode TENG, indicating the simultaneous production of AC and DC output.

Furthermore, Li et al. (2020a) reported a self-powered vibration sensor system and achieved real-time and continuous detection of the vibration characteristics from an AC/DC-TENG. The detailed structure is shown in Figure 14B(i). When the slider moves beyond the safe zone and into the dangerous zone, a high electrostatic field will be built between the CCE and the charged triboelectric layer, and the air will be ionized with a DC output in external circuit and driving the alarm light directly. Alike with the conventional AC-TENG, the output AC signal contains the moving information, such as amplitude, frequency, velocity, and acceleration, which can be used for a motion sensor. More importantly, instead of judging the position by the signal amplitude, the AC/DC-TENG can precisely judge the vibration amplitude by using the signal type changed from AC to DC (Figure 14B(ii)). In addition, this self-powered vibration sensor system can realize real-time feedback by detecting the signal type changes from AC to DC, and using DC output drives an alarm system directly, which provides a convenient and effective avenue for monitoring the structural health of construction.

SUMMARY AND PERSPECTIVES

Ever since the invention of TENG in 2012, it has attracted significant attention as an emerging mechanical energy harvesting technology and has drawn broad interest across different research communities, such as energy science, self-powered sensors, wearable electronics, robotics, environmental sciences, implantable devices, and artificial intelligence. The studies of TENG greatly promote the understanding of the physical mechanism of CE. With the huge progress of TENG from fundamental physics to optimization of output performance, the applications of TENG are mainly in four major fields including micro/nano power source for small and mobile electronics, self-powered system as an active sensor, integrating many units of TENGs into a network to harvest large-scale blue energy, and high-voltage power source for specific high-voltage application (Figure 15) (Wu et al., 2019). Although the roadmap is drawn for the AC-TENG, it is still suitable

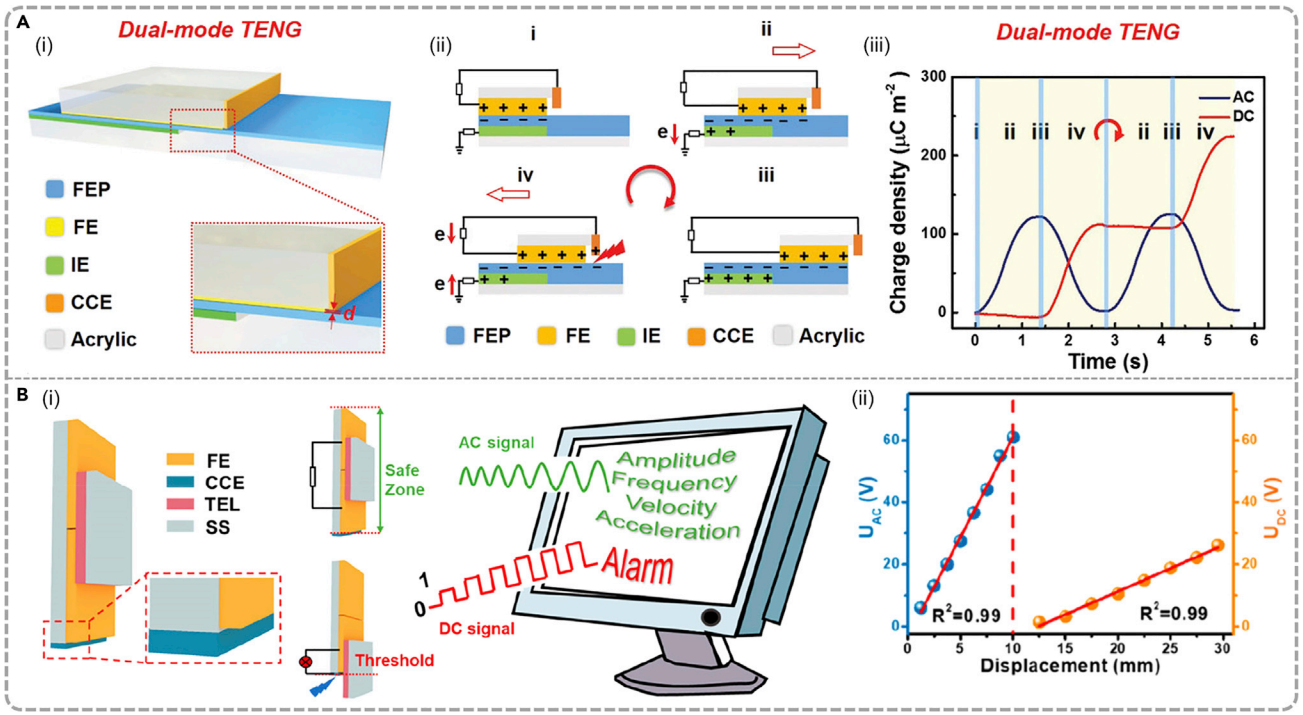

Figure 14. Dual-mode TENG

(A) (i) The schematic diagram of sliding dual-mode TENG composed of an AC-TENG and a DC-TENG. (ii) The working mechanism and (iii) output charge density of the dual-mode TENG. Adopted from (Zhou et al., 2020a).

(B) (i) The schematic illustration of AC/DC-TENG as a fully self-powered vibration monitoring sensor. (ii) The typical output voltage of the AC/DC-TENG in monitoring vibration motion by using the signal type changed from AC to DC. Adopted from (Li et al., 2020a).

for DC-TENG. Reviewing the development of TENG, AC-TENG is developing along the roadmap, and we think that the development of DC-TENG will continue to follow the roadmap.

Although great achievements have been realized in AC-TENG, there are still some issues to be resolved for its large-scale commercial applications, including fundamental physics of TE, high-performance triboelectric materials, durability of the materials and devices, packaging technology for preventing environmental factors including moisture and atmosphere, system integration, and environmental interaction, which are discussed in detail in a recent review (Wu et al., 2019).

In terms of the efficiency of energy storage and powering electronics, DC output is more favorable. Generally, a power management system is always needed to convert AC to DC output for powering electronics. While those electronic components can realize the regulation and control of the output electric signal to some extent, the used electronic elements, such as the rectifier, transformer, transistor, inductor, and energy storage unit, need to consume a part of energy and then reduce the whole energy conversion efficiency. Therefore, the high-efficiency power management system with a wearable, portable, and flexible manner needs to be further exploited in future. By using phase control, the crest factor of output current obtained by mechanical rectifier can be tuned; however, the precise phase control is a problem to achieve a constant current output, and the durability in sliding-type TENG is also needed to be improved for practical application.

Compared with the relatively matured research field of AC-TENG from electrostatic induction, the research of DC-TENG arising from electrostatic breakdown is just beginning, and there are still many problems to be resolved for the development of DC-TENG, especially the very meaningful constant current TENG. Until now, some achievements have been realized. A primary physics model of the DC-TENG has been proposed for understanding the process of power output (Xu et al., 2020b). For mechanical energy harvesting, the lateral sliding mode and rotary mode DC-TENG has been achieved for effectively converting

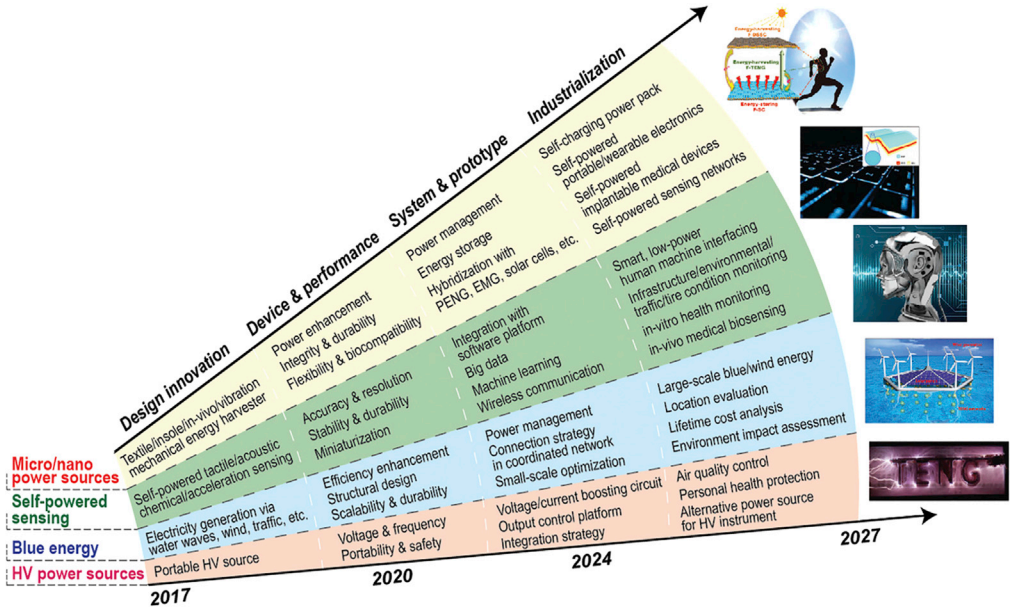

Figure 15. The roadmap of TENG from 2017 to 2027
Adopted from (Wu et al., 2019)

mechanical energy into DC output or constant current output, and a DC-TENG based on fabric has been demonstrated in a recent work for bio-motion energy harvesting (Chen et al., 2020a). In terms of sensing applications, a motion vector sensor has been realized to measure various motion parameters and even realized motion trajectory tracing, mapping, and writing on the curved surface (Yin et al., 2020). Furthermore, the effects of atmospheric pressure and temperature on the output performance of DC-TENG have been studied, which can simultaneously harvest mechanical and thermal energy in a single device (Liu et al., 2020b). The DC-TENG has shown its significant potential in energy harvesting and sensors, but there are several issues and problems that need to be addressed, as listed in the following:

(1) The fundamental physics of AC-TENG is the displacement current, whereas the air discharge part of DC-TENG is conduction current, but it is unclear whether the TE part of DC-TENG can be understood by the displacement current. If not, the special fundamental physics of DC-TENG needs to be exploited. Besides, the electrostatic induction process in AC-TENG has been revealed by theoretical investigation in depth (Niu and Wang, 2015; Shao et al., 2019b, 2020); however, the theoretical study of electrostatic breakdown process in DC-TENG needs to be addressed in the following investigation.

(2) The FOMs are highly desired for evaluating the output performance of DC-TENG, which may refer to the FOMs of AC-TENG. As an energy harvester, the commercialization and application of DC-TENGs highly depends on its power density, which is quadratically related to the effective charge density. DC-TENG converts the sliding-mode electrification of per cycle to breakdown energy, which is different from the conventional AC-TENG that can reach a high surface charge density by an accumulation process during multiple cycles. Therefore, the triboelectric layer with higher amount of charge transfer in one cycle is preferable for high-performance DC-TENG.

(3) The working mechanism of DC-TENG is based on the TE effect and the electrostatic breakdown between the charged surface and the CCE, which is free from the limitation of $\sigma_{\text{dielectric breakdown}}$ in AC-TENG. Therefore, the limitation of its effective surface charge density ($\sigma_{\text{DC-TENG}}$) can be described as

$$\sigma_{\text{DC-TENG}} = \min\left(\sigma_{\text{triboelectrification}}, \sigma_{\text{c, electrostatic breakdown}}\right) \quad \text{(Equation 4)}$$

where $\sigma_{\text{c, electrostatic breakdown}}$ represents the collected charge density by electrostatic breakdown. Therefore, besides improving the process of TE such as material modification, effective contact and

Table 1. A comparison of AC-TENG and DC-TENG

	Alternating current triboelectric nanogenerator (AC-TENG)		Direct current triboelectric nanogenerator (DC-TENG)	
	Contact-separation-type (Contact-separation and single-electrode modes)	Sliding-type (sliding and free-standing modes)	DC-TENG from electrostatic induction with mechanical rectifier	DC-TENG from electrostatic breakdown (sliding mode)
Mechanism	• Contact electrification and electrostatic induction • Maxwell's displacement current			• Contact electrification and electrostatic breakdown • Conduction current
Physical model	• An electric charge source and a variable capacitor			• An electric charge source and a broken down capacitor
Output	• Alternative current		• Direct current	• Constant current
Pros	• Easy to get high charge density by charge accumulation process • Wireless transmission • High durability	• Easy to get high charge density by charge accumulation process • Wireless transmission	• Easy to get high charge density by charge accumulation process • No need to rectify	• Constant current source[a] • No need to rectify • Not restricted by dielectric breakdown[b]
Cons	• Needs rectification • Restricted by dielectric breakdown	• Needs rectification • Restricted by dielectric breakdown • Low durability[c]	• Complex structure • Restricted by dielectric breakdown	• Without charge accumulation process • No wireless transmission • Low durability[c]
Optimizing methods	• Improving surface charge density (triboelectrification, ion-injection, charge pumping) • Avoiding gas breakdown (high atmospheric pressure, high vacuum, ultra-thin triboelectric layer)			• Improving triboelectrification process • Enhancing gas breakdown (microstructure, high temperature, low atmospheric pressure)

[a]The output current keeps nearly stable from zero to several tens of megaohm resistance.
[b]The DC-TENG from electrostatic breakdown is free from the limitation of $\sigma_{\text{dielectric breakdown}}$ in AC-TENG, so the ultimate charge density of DC-TENG is higher than conventional AC-TENG.
[c]Introducing interface liquid lubrication between the triboelectric layers has been reported to greatly enhance the durability of sliding-type TENG.

environmental control similar to conventional AC-TENG, from a new angle to enhance the process of electrostatic breakdown such as structural design and environmental control, is also highly desired.

(4) To promote the practical application of the DC-TENG, the durability induced by violent friction during sliding process is one of the key concerns. The possible solutions such as introducing interface liquid lubrication (Zhou et al., 2020c) and developing new materials or structures that have the most robust mechanical durability and stability are suggested.

For better understanding the particular characteristics of the AC-TENG and DC-TENG, a comparison between AC-TENG and DC-TENG is presented in Table 1 from their mechanism, physical model, output characteristics, advantages, and disadvantages to optimizing methods. In a word, the AC-TENG has the advantages of ease of realizing high charge density by charge accumulation process and wireless transmission, whereas DC-TENG has the advantages of constant current output and higher theoretical charge density without the limitation of dielectric breakdown.

As for AC/DC-TENG, it shows particular superiority in mechanical energy harvesting and self-powered systems when compared with the single-mode TENG. By rationally designing the structure of TENGs, the final energy output can be enhanced without increasing the whole device size by integrating the AC-TENG and DC-TENG. According to the different characteristics of AC and DC output, AC/DC-TENG can be used to precisely judge the vibration amplitude by using the signal type changes from AC to DC, instead of judging the position only by the signal amplitude, which is like the 0-1 binary code signals in computer programming. In addition, this self-powered vibration sensor system can realize real-time feedback by detecting

the signal type changes from AC to DC and using DC output drives an alarm system directly, which provides a convenient and effective avenue for monitoring the structural health of construction. The applications of dual-mode TENG in sensors will be a new research direction. However, it still requires new structural design to skillfully combine electrostatic induction and electrostatic breakdown in principle to maximize the final energy output.

Exploring the full potential of TENG from new structures to realize DC output is highly desired for accelerating the miniaturization of IoTs and self-powered systems and may promote the understanding of TENG and CE from a new horizon. Besides the above-mentioned DC-TENG, there are still other DC generators have been reported based on Schottky knot, silicon p-n junction, contact barrier between metal and semiconductor, and tunneling effect in metal-insulator-semiconductor structure (Lin et al., 2019; Liu et al., 2018a, 2018b, 2019b; Lu et al., 2019; Shao et al., 2019a; Xu et al., 2019a; Zhang et al., 2018a, 2018b, 2020c), in which the most basic mechanism for charge transfer is still CE. These generators can be considered as the general DC-TENG. In a word, the DC output of TENG can be achieved not only by electric rectifier, mechanical rectifier, air breakdown, and electric potential barrier but also by other methods to limit the direction of electron flow to realize a DC output.

Resource availability

Lead contact

Further information and requests for resources should be directly to and will be fulfilled by the Lead Contact, Jie Wang, wangjie@binn.cas.cn.

Materials availability

This study did not generate any new unique reagents.

Data and code availability

This review did not generate datasets or analyze codes.

ACKNOWLEDGMENTS

This research was supported by the National Key R & D Project from Minister of Science and Technology (2016YFA0202704), National Natural Science Foundation of China (Grant No. 61774016, 21773009, 51432005, 5151101243, 51561145021). The authors thank our group members and collaborators for their contribution to the development of TENG.

AUTHOR CONTRIBUTIONS

D.L., L.Z., J.W., and Z.L.W. conceived the idea, wrote the paper, and prepared the figures. All the authors discussed the results and commented on the manuscript.

REFERENCES

An, J., Wang, Z.M., Jiang, T., Liang, X., and Wang, Z.L. (2019). Whirling-folded triboelectric nanogenerator with high average power for water wave energy harvesting. Adv. Funct. Mater. *29*, 1904867.

Chen, C.Y., Guo, H.Y., Chen, L.J., Wang, Y.C., Pu, X.J., Yu, W.D., Wang, F.M., Du, Z.Q., and Wang, Z.L. (2020a). Direct current fabric triboelectric nanogenerator for biomotion energy harvesting. ACS Nano *14*, 4585–4594.

Chen, J., Guo, H.Y., Hu, C.G., and Wang, Z.L. (2020b). Robust triboelectric nanogenerator achieved by centrifugal force induced automatic working mode transition. Adv. Energy Mater. *10*, 2000886.

Cheng, J., Ding, W.B., Zi, Y.L., Lu, Y.J., Ji, L.H., Liu, F., Wu, C.S., and Wang, Z.L. (2018a). Triboelectric microplasma powered by mechanical stimuli. Nat. Commun. *9*, 3733.

Cheng, L., Xu, Q., Zheng, Y.B., Jia, X.F., and Qin, Y. (2018b). A self-improving triboelectric nanogenerator with improved charge density and increased charge accumulation speed. Nat. Commun. *9*, 3773.

Chun, J.S., Ye, B.U., Lee, J.W., Choi, D., Kang, C.Y., Kim, S.W., Wang, Z.L., and Baik, J.M. (2016). Boosted output performance of triboelectric nanogenerator via electric double layer effect. Nat. Commun. *7*, 12985.

Dharmasena, R.D.I.G., Cronin, H.M., Dorey, R.A., and Silva, S.R.P. (2020). Direct current contact-mode triboelectric nanogenerators via systematic phase shifting. Nano Energy *75*, 104887.

Fan, F.R., Tian, Z.Q., and Wang, Z.L. (2012). Flexible triboelectric generator! Nano Energy *1*, 328–334.

Guo, H.Y., Pu, X.J., Chen, J., Meng, Y., Yeh, M.H., Liu, G.L., Tang, Q., Chen, B.D., Liu, D., Qi, S., et al. (2018). A highly sensitive, self-powered triboelectric auditory sensor for social robotics and hearing aids. Sci. Robot. *3*, eaat2516.

Han, K., Luo, J.J., Feng, Y.W., Xu, L., Tang, W., and Wang, Z.L. (2020). Self-powered electrocatalytic ammonia synthesis directly from air as driven by dual triboelectric nanogenerators. Energy Environ. Sci. *13*, 2450–2458.

Harmon, W., Bamgboje, D., Guo, H.Y., Hu, T.S., and Wang, Z.L. (2020). Self-driven power management system for triboelectric nanogenerators. Nano Energy *71*, 104642.

He, W.C., Liu, W.L., Chen, J., Wang, Z., Liu, Y.K., Pu, X.J., Yang, H.M., Tang, Q., Yang, H.K., Guo, H.Y., et al. (2020). Boosting output performance of sliding mode triboelectric nanogenerator by

charge space-accumulation effect. Nat. Commun. *11*, 4277.

Huang, D.C., Shu, Y.B., Ruan, J.J., and Hu, Y. (2009). Ultra high voltage transmission in China: developments, current status and future prospects. Proc. IEEE *97*, 555–583.

Kim, T., Kim, D.Y., Yun, J., Kim, B., Lee, S.H., Kim, D., and Lee, S. (2018). Direct-current triboelectric nanogenerator via water electrification and phase control. Nano Energy *52*, 95–104.

Larcher, D., and Tarascon, J.M. (2015). Towards greener and more sustainable batteries for electrical energy storage. Nat. Chem. *7*, 19–29.

Li, A.Y., Zi, Y.L., Guo, H.Y., Wang, Z.L., and Fernandez, F.M. (2017). Triboelectric nanogenerators for sensitive nano-coulomb molecular mass spectrometry. Nat. Nanotechnol. *12*, 481–487.

Li, S.M., Wang, S.H., Zi, Y.L., Wen, Z., Lin, L., Zhang, G., and Wang, Z.L. (2015). Largely improving the robustness and lifetime of triboelectric nanogenerators through automatic transition between contact and noncontact working states. ACS Nano *9*, 7479–7487.

Li, S.M., Zhou, Y.S., Zi, Y.L., Zhang, G., and Wang, Z.L. (2016). Excluding contact electrification in surface potential measurement using kelvin probe force microscopy. ACS Nano *10*, 2528–2535.

Li, S.X., Liu, L., Zhao, Z.H., Zhou, L.L., Yin, X., Li, X.Y., Gao, Y.K., Zhang, C.G., Zhang, Q., Wang, J., et al. (2020b). A fully self-powered vibration monitoring system driven by dual-mode triboelectric nanogenerators. ACS Nano *14*, 2475–2482.

Li, X.Y., Yin, X., Zhao, Z.H., Zhou, L.L., Liu, D., Zhang, C.L., Zhang, C.G., Zhang, W., Li, S.X., Wang, J., et al. (2020c). Long-lifetime triboelectric nanogenerator operated in conjunction modes and low crest factor. Adv. Energy Mater. *10*, 1903024.

Lin, L., Wang, S.H., Xie, Y.N., Jing, Q.S., Niu, S.M., Hu, Y.F., and Wang, Z.L. (2013). Segmentally structured disk triboelectric nanogenerator for harvesting rotational mechanical energy. Nano Lett. *13*, 2916–2923.

Lin, S.S., Lu, Y.H., Feng, S.R., Hao, Z.Z., and Yan, Y.F. (2019). A high current density direct-current generator based on a moving van der waals Schottky diode. Adv. Mater. *31*, 1804398.

Lin, S.Q., Xu, C., Xu, L., and Wang, Z.L. (2020a). The overlapped electron-cloud model for electron transfer in contact electrification. Adv. Funct. Mater. *30*, 1909724.

Lin, S.Q., Xu, L., Wang, A.C., and Wang, Z.L. (2020b). Quantifying electron-transfer in liquid-solid contact electrification and the formation of electric double-layer. Nat. Commun. *11*, 399.

Lin, Z.H., Cheng, G., Lee, S., Pradel, K.C., and Wang, Z.L. (2014). Harvesting water drop energy by a sequential contact-electrification and electrostatic-induction process. Adv. Mater. *26*, 1400373.

Liu, D., Bao, J.F., Chen, Y.L., Li, G.K., and Zhang, X.S. (2020a). Unidirectional-current triboelectric nanogenerator based on periodical lateral-cantilevers. Nano Energy *74*, 104770.

Liu, D., Yin, X., Guo, H.Y., Zhou, L.L., Li, X.Y., Zhang, C.L., Wang, J., and Wang, Z.L. (2019a). A constant current triboelectric nanogenerator arising from electrostatic breakdown. Sci. Adv. *5*, eaav6437.

Liu, D., Zhou, L.L., Li, S.X., Zhao, Z.H., Yin, X., Yi, Z.Y., Zhang, C.L., Li, X.Y., Wang, J., and Wang, Z.L. (2020b). Hugely enhanced output power of direct-current triboelectric nanogenerators by using electrostatic breakdown effect. Adv. Mater. Technol. *5*, 2000289.

Liu, J., Goswami, A., Jiang, K., Khan, F., Kim, S., McGee, R., Li, Z., Hu, Z., Lee, J., and Thundat, T. (2018a). Direct-current triboelectricity generation by a sliding Schottky nanocontact on MoS_2 multilayers. Nat. Nanotechnol. *13*, 112–116.

Liu, J., Liu, F., Bao, R., Jiang, K., Khan, F., Li, Z., Peng, H., Chen, J., Alodhayb, A., and Thundat, T. (2019b). Scaled-up direct-current generation in MoS_2 multilayer-based moving heterojunctions. ACS Appl. Mater. Interfaces *11*, 35404–35409.

Liu, J., Miao, M., Jiang, K., Khan, F., Goswami, A., McGee, R., Li, Z., Nguyen, L., Hu, Z., Lee, J., et al. (2018b). Sustained electron tunneling at unbiased metal-insulator-semiconductor triboelectric contacts. Nano Energy *48*, 320–326.

Liu, W.L., Wang, Z., Wang, G., Liu, G.L., Chen, J., Pu, X.J., Xi, Y., Wang, X., Guo, H.Y., Hu, C.G., et al. (2019c). Integrated charge excitation triboelectric nanogenerator. Nat. Commun. *10*, 1426.

Liu, Y.K., Liu, W.L., Wang, Z., He, W.C., Tang, Q., Xi, Y., Wang, X., Guo, H.Y., and Hu, C.G. (2020c). Quantifying contact status and the air-breakdown model of charge-excitation triboelectric nanogenerators to maximize charge density. Nat. Commun. *11*, 1599.

Lu, Y.G., Hao, Z.Z., Feng, S.R., Shen, R.J., Yan, Y.F., and Lin, S.S. (2019). Direct-current generator based on dynamic PN junctions with the designed voltage output. iScience *22*, 58–69.

Luo, J.J., Wang, Z.M., Xu, L., Wang, A.C., Han, K., Jiang, T., Lai, Q.S., Bai, Y., Tang, W., Fan, F.R., et al. (2019). Flexible and durable wood-based triboelectric nanogenerators for self-powered sensing in athletic big data analytics. Nat. Commun. *10*, 5147.

Luo, J.J., Xu, L., Tang, W., Jiang, T., Fan, F.R., Pang, Y.K., Chen, L.B., Zhang, Y., and Wang, Z.L. (2018). Direct-current triboelectric nanogenerator realized by air breakdown induced ionized air channel. Adv. Energy Mater. *8*, 1800889.

Ma, L.Y., Wu, R.H., Liu, S., Patil, A., Gong, H., Yi, J., Sheng, F.F., Zhang, Y.Z., Wang, J., Wang, J., et al. (2020). A machine-fabricated 3D honeycomb-structured flame-retardant triboelectric fabric for fire escape and rescue. Adv. Mater. *32*, 2003897.

Nie, J.H., Ren, Z.W., Shao, J.J., Deng, C.R., Xu, L., Chen, X.Y., Li, M.C., and Wang, Z.L. (2018). Self-powered microfluidic transport system based on triboelectric nanogenerator and electrowetting technique. ACS Nano *12*, 1491–1499.

Niu, S.M., Liu, Y., Wang, S.H., Lin, L., Zhou, Y.S., Hu, Y.F., and Wang, Z.L. (2014). Theoretical investigation and structural optimization of single-electrode triboelectric nanogenerators. Adv. Funct. Mater. *24*, 3332–3340.

Niu, S.M., Wang, X.F., Yi, F., Zhou, Y.S., and Wang, Z.L. (2015). A universal self-charging system driven by random biomechanical energy for sustainable operation of mobile electronics. Nat. Commun. *6*, 8975.

Niu, S.M., and Wang, Z.L. (2015). Theoretical systems of triboelectric nanogenerators. Nano Energy *14*, 161–192.

Ouyang, H., Liu, Z., Li, N., Shi, B.J., Zou, Y., Xie, F., Ma, Y., Li, Z., Li, H., Zheng, Q., et al. (2019). Symbiotic cardiac pacemaker. Nat. Commun. *10*, 1821.

Peng, F., Liu, D., Zhao, W., Zheng, G.Q., Ji, Y.X., Dai, K., Mi, L.W., Zhang, D.B., Liu, C.T., and Shen, C.Y. (2019). Facile fabrication of triboelectric nanogenerator based on low-cost thermoplastic polymeric fabrics for large-area energy harvesting and self-powered sensing. Nano Energy *65*, 104068.

Peng, X., Dong, K., Ye, C.Y., Jiang, Y., Zhai, S.Y., Cheng, R.W., Liu, D., Gao, X.P., Wang, J., and Wang, Z.L. (2020). A breathable, biodegradable, antibacterial, and self-powered electronic skin based on all-nanofiber triboelectric nanogenerators. Sci. Adv. *6*, eaba9624.

Pingali, K.C., Hammond, S.V., Muzzio, F.J., and Shinbrot, T. (2009). Use of a static eliminator to improve powder flow. Int. J. Pharma. *369*, 2–4.

Pu, X., Liu, M.M., Chen, X.Y., Sun, J.M., Du, C.H., Zhang, Y., Zhai, J.Y., Hu, W.G., and Wang, Z.L. (2017a). Ultrastretchable, transparent triboelectric nanogenerator as electronic skin for biomechanical energy harvesting and tactile sensing. Sci. Adv. *3*, e1700015.

Pu, X.J., Guo, H.Y., Chen, J., Wang, X., Xi, Y., Hu, C.G., and Wang, Z.L. (2017b). Eye motion triggered self-powered mechnosensational communication system using triboelectric nanogenerator. Sci. Adv. *3*, e1700694.

Pu, Y., Mazumder, M., and Cooney, C. (2009). Effects of electrostatic charging on pharmaceutical powder blending homogeneity. J. Pharm. Sci. *98*, 2412–2421.

Qiao, G., Wang, J., Yu, X., Jia, R., Cheng, T., and Wang, Z.L. (2021). A bidirectional direct current triboelectric nanogenerator with the mechanical rectifier. Nano Energy *79*, 105408.

Qin, H., Cheng, G., Zi, Y., Gu, G., Zhang, B., Shang, W., Yang, F., Yang, J., Du, Z., and Wang, Z.L. (2018). High energy storage efficiency triboelectric nanogenerators with unidirectional switches and passive power management circuits. Adv. Funct. Mater. *28*, 1805216.

Ryu, H., Lee, J.H., Khan, U., Kwak, S.S., Hinchet, R., and Kim, S.W. (2018). Sustainable direct current powering a triboelectric nanogenerator via a novel asymmetrical design. Energy Environ. Sci. *11*, 2057–2063.

Salama, F., Sowinski, A., Atieh, K., and Mehrani, P. (2013). Investigation of electrostatic charge distribution within the reactor wall fouling and bulk regions of a gas-solid fluidized bed. J. Electrostat. *71*, 21–27.

Sayfidinov, K., Cezan, S.D., Baytekin, B., and Baytekin, H.T. (2018). Minimizing friction, wear, and energy losses by eliminating contact charging. Sci. Adv. *4*, eaau3808.

Shao, H., Fang, J., Wang, H., Niu, H., Zhou, H., Cao, Y., Chen, F., Fu, S., and Lin, T. (2019a). Schottky direct-current energy harvesters with large current output density. Nano Energy *62*, 171–180.

Shao, J.J., Jiang, T., and Wang, Z.L. (2020). Theoretical foundations of triboelectric nanogenerators (TENGs). Sci. China Technol. Sci. *63*, 1087–1109.

Shao, J.J., Willatzen, M., Jiang, T., Tang, W., Chen, X.Y., Wang, J., and Wang, Z.L. (2019b). Quantifying the power output and structural figure-of-merits of triboelectric nanogenerators in a charging system starting from the Maxwell's displacement current. Nano Energy *59*, 380–389.

Shaw, P.E. (1926). The electrical charges from like solids. Nature *118*, 659–660.

Song, W.X., Yin, X., Liu, D., Ma, W.T., Zhang, M.Q., Li, X.Y., Cheng, P., Zhang, C.L., Wang, J., and Wang, Z.L. (2019). A highly elastic self-charging power system for simultaneously harvesting solar and mechanical energy. Nano Energy *65*, 103997.

Wang, H.M., Xu, L., Bai, Y., and Wang, Z.L. (2020a). Pumping up the charge density of a triboelectric nanogenerator by charge-shuttling. Nat. Commun. *11*, 4203.

Wang, J., Li, S.M., Yi, F., Zi, Y.L., Lin, J., Wang, X.F., Xu, Y.L., and Wang, Z.L. (2016a). Sustainably powering wearable electronics solely by biomechanical energy. Nat. Commun. *7*, 12744.

Wang, J., Li, Y., Xie, Z., Xu, Y., Zhou, J., Cheng, T., Zhao, H., and Wang, Z.L. (2020b). Cylindrical direct-current triboelectric nanogenerator with constant output current. Adv. Energy Mater. *10*, 1904227.

Wang, J., Wu, C.S., Dai, Y.J., Zhao, Z.H., Wang, A., Zhang, T.J., and Wang, Z.L. (2017). Achieving ultrahigh triboelectric charge density for efficient energy harvesting. Nat. Commun. *8*, 88.

Wang, J., Wu, Z., Pan, L., Gao, R., Zhang, B., Yang, L., Guo, H., Liao, R., and Wang, Z.L. (2019). Direct-current rotary-tubular triboelectric nanogenerators based on liquid-dielectrics contact for sustainable energy harvesting and chemical composition analysis. ACS Nano *13*, 2587–2598.

Wang, S.H., Xie, Y.N., Niu, S.M., Lin, L., Liu, C., Zhou, Y.S., and Wang, Z.L. (2014a). Maximum surface charge density for triboelectric nanogenerators achieved by ionized-air injection: methodology and theoretical understanding. Adv. Mater. *26*, 6720–6728.

Wang, S.H., Xie, Y.N., Niu, S.M., Lin, L., and Wang, Z.L. (2014b). Freestanding triboelectric-layer-based nanogenerators for harvesting energy from a moving object or human motion in contact and non-contact modes. Adv. Mater. *26*, 2818–2824.

Wang, S.H., Zi, Y.L., Zhou, Y.S., Li, S.M., Fan, F.R., Lin, L., and Wang, Z.L. (2016b). Molecular surface functionalization to enhance the power output of triboelectric nanogenerators. J. Mater. Chem. A *4*, 3728–3734.

Wang, Z.L. (2014). Triboelectric nanogenerators as new energy technology and self-powered sensors-principles, problems and perspectives. Faraday Discuss. *176*, 447–458.

Wang, Z.L. (2017). On Maxwell's displacement current for energy and sensors: the origin of nanogenerators. Mater. Today *20*, 74–82.

Wang, Z.L. (2019). Entropy theory of distributed energy for internet of things. Nano Energy *58*, 669–672.

Wang, Z.L. (2020a). On the first principle theory of nanogenerators from Maxwell's equations. Nano Energy *68*, 104272.

Wang, Z.L. (2020b). Triboelectric nanogenerator (TENG)-sparking an energy and sensor revolution. Adv. Energy Mater. *10*, 2000137.

Wang, Z.L., and Wang, A.C. (2019). On the origin of contact-electrification. Mater. Today *30*, 34–51.

Wang, Z.M., An, J., Nie, J.H., Luo, J.J., Shao, J.J., Jiang, T., Chen, B.D., Tang, W., and Wang, Z.L. (2020c). A self-powered angle sensor at nanoradian-resolution for robotic arms and personalized medicare. Adv. Mater. *32*, 2001466.

Wu, C.S., Ding, W.B., Liu, R.Y., Wang, J.Y., Wang, A.C., Wang, J., Li, S.M., Zi, Y.L., and Wang, Z.L. (2018). Keystroke dynamics enabled authentication and identification using triboelectric nanogenerator array. Mater. Today *21*, 216–222.

Wu, C.S., Wang, A.C., Ding, W.B., Guo, H.Y., and Wang, Z.L. (2019). Triboelectric nanogenerator: a foundation of the energy for the new era. Adv. Energy Mater. *9*, 1802906.

Xi, F.B., Pang, Y.K., Li, W., Jiang, T., Zhang, L.M., Guo, T., Liu, G.X., Zhang, C., and Wang, Z.L. (2017). Universal power management strategy for triboelectric nanogenerator. Nano Energy *37*, 168–176.

Xiong, J.Q., Thangavel, G., Wang, J.X., Zhou, X.R., and Lee, P.S. (2020). Self-healable sticky porous elastomer for gas-solid interacted power generation. Sci. Adv. *6*, eabb4246.

Xu, G.Q., Guan, D., Yin, X., Fu, J.J., Wang, J., and Zi, Y.L. (2020a). A coplanar-electrode direct-current triboelectric nanogenerator with facile fabrication and stable output. EcoMat *2*, e12037.

Xu, L., Bu, T.Z., Yang, X.D., Zhang, C., and Wang, Z.L. (2018). Ultrahigh charge density realized by charge pumping at ambient conditions for triboelectric nanogenerators. Nano Energy *49*, 625–633.

Xu, R., Zhang, Q., Wang, J.Y., Liu, D., Wang, J., and Wang, Z.L. (2019a). Direct current triboelectric cell by sliding an n-type semiconductor on a p-type semiconductor. Nano Energy *66*, 104185.

Xu, S., Guo, H., Zhang, S.L., Jin, L., Ding, W., Wang, X., and Wang, Z.L. (2020b). Theoretical investigation of air breakdown direct current triboelectric nanogenerator. Appl. Phys. Lett. *116*, 263901.

Xu, S.X., Ding, W.B., Guo, H.Y., Wang, X.H., and Wang, Z.L. (2019b). Boost the performance of triboelectric nanogenerators through circuit oscillation. Adv. Energy Mater. *9*, 1900772.

Yang, H., Pang, Y.K., Bu, T.Z., Liu, W.B., Luo, J.J., Jiang, D.D., Zhang, C., and Wang, Z.L. (2019). Triboelectric micromotors actuated by ultralow frequency mechanical stimuli. Nat. Commun. *10*, 2309.

Yang, Y., Zhang, H.L., and Wang, Z.L. (2014). Direct-current triboelectric generator. Adv. Funct. Mater. *24*, 3745–3750.

Yang, Y., Zhou, Y.S., Zhang, H.L., Liu, Y., Lee, S.M., and Wang, Z.L. (2013). A single-electrode based triboelectric nanogenerator as self-powered tracking system. Adv. Mater. *25*, 6594–6601.

Yin, X., Liu, D., Zhou, L.L., Li, X.Y., Xu, G.Q., Liu, L., Li, S.X., Zhang, C.G., Wang, J., and Wang, Z.L. (2020). A motion vector sensor via direct-current triboelectric nanogenerator. Adv. Funct. Mater. *30*, 2002547.

Yin, X., Liu, D., Zhou, L.L., Li, X.Y., Zhang, C.L., Cheng, P., Guo, H.Y., Song, W.X., Wang, J., and Wang, Z.L. (2019). Structure and dimension effects on the performance of layered triboelectric nanogenerators in contact-separation mode. ACS Nano *13*, 698–705.

Yoon, H.J., Kang, M., Seung, W., Kwak, S.S., Kim, J., Kim, H.T., and Kim, S.W. (2020). Microdischarge-based direct current triboelectric nanogenerator via accumulation of triboelectric charge in atmospheric condition. Adv. Energy Mater. *10*, 2000730.

Zhang, C., Zhou, T., Tang, W., Han, C., Zhang, L., and Wang, Z.L. (2014). Rotating-disk-based direct-current triboelectric nanogenerator. Adv. Energy Mater. *4*, 1301798.

Zhang, C.L., Zhou, L.L., Cheng, P., Yin, X., Liu, D., Li, X.Y., Guo, H.Y., Wang, Z.L., and Wang, J. (2020a). Surface charge density of triboelectric nanogenerators: theoretical boundary and optimization methodology. Appl. Mater. Today *18*, 100496.

Zhang, H.M., Marty, F., Xia, X., Zi, Y.L., Bourouina, T., Galayko, D., and Basset, P. (2020b). Employing a MEMS plasma switch for conditioning high-voltage kinetic energy harvesters. Nat. Commun. *11*, 3221.

Zhang, Q., Xu, R., and Cai, W. (2018a). Pumping electrons from chemical potential difference. Nano Energy *51*, 698–703.

Zhang, X.S., Han, M.D., Kim, B., Bao, J.F., Brugger, J., and Zhang, H.X. (2018b). All-in-one self-powered flexible microsystems based on triboelectric nanogenerators. Nano Energy *47*, 410–426.

Zhang, Z., Jiang, D.D., Zhao, J.Q., Liu, G.X., Bu, T.Z., Zhang, C., and Wang, Z.L. (2020c). Tribovoltaic effect on metal-semiconductor interface for direct-current low-impedance triboelectric nanogenerators. Adv. Energy Mater. *10*, 1903713.

Zhou, L.L., Liu, D., Li, S.X., Zhao, Z.H., Zhang, C.L., Yin, X., Liu, L., Cui, S.N., Wang, Z.L., and Wang, J. (2020a). Rationally designed dual-mode triboelectric nanogenerator for harvesting

mechanical energy by both electrostatic induction and dielectric breakdown effects. Adv. Energy Mater. *10*, 2000965.

Zhou, L.L., Liu, D., Li, S.X., Yin, X., Zhang, C.L., Li, X.Y., Zhang, C.G., Zhang, W., Cao, X., Wang, J., et al. (2019). Effective removing of hexavalent chromium from wasted water by triboelectric nanogenerator driven self-powered electrochemical system - why pulsed DC is better than continuous DC? Nano Energy *64*, 103915.

Zhou, L.L., Liu, D., Wang, J., and Wang, Z.L. (2020b). Triboelectric nanogenerators: fundamental physics and potential applications. Friction *8*, 481–506.

Zhou, L.L., Liu, D., Zhao, Z.H., Li, S.X., Liu, Y.B., Liu, L., Gao, Y.K., Wang, Z.L., and Wang, J. (2020c). Simultaneously enhancing power density and durability of sliding-mode triboelectric nanogenerator via interface liquid lubrication. Adv. Energy Mater. https://doi.org/10.1002/aenm.202002920.

Zhou, Y.S., Li, S.M., Niu, S.M., and Wang, Z.L. (2016). Effect of contact- and sliding-mode electrification on nanoscale charge transfer for energy harvesting. Nano Res. *9*, 3705–3713.

Zhu, G., Chen, J., Zhang, T.J., Jing, Q.S., and Wang, Z.L. (2014a). Radial-arrayed rotary electrification for high performance triboelectric generator. Nat. Commun. *5*, 3426.

Zhu, G., Pan, C.F., Guo, W.X., Chen, C.Y., Zhou, Y.S., Yu, R.M., and Wang, Z.L. (2012). Triboelectric-generator-driven pulse electrodeposition for micropatterning. Nano Lett. *12*, 4960–4965.

Zhu, G., Zhou, Y.S., Bai, P., Meng, X.S., Jing, Q.S., Chen, J., and Wang, Z.L. (2014b). A shape-adaptive thin-film-based approach for 50% high-efficiency energy generation through micro-grating sliding electrification. Adv. Mater. *26*, 3788–3796.

Zhu, J., Wang, H., Zhang, Z., Ren, Z., Shi, Q., Liu, W., and Lee, C. (2020). Continuous direct current by charge transportation for next-generation IoT and real-time virtual reality applications. Nano Energy *73*, 104760.

Zi, Y.L., Niu, S.M., Wang, J., Wen, Z., Tang, W., and Wang, Z.L. (2015). Standards and figure-of-merits for quantifying the performance of triboelectric nanogenerators. Nat. Commun. *6*, 8376.

Zi, Y.L., Wu, C.S., Ding, W.B., and Wang, Z.L. (2017). Maximized effective energy output of contact-separationtriggered triboelectric nanogenerators as limited by air breakdown. Adv. Funct. Mater. *27*, 1700049.

Zou, H.Y., Guo, L.T., Xue, H., Zhang, Y., Shen, X.F., Liu, X.T., Wang, P.H., He, X., Dai, G.Z., Jiang, P., et al. (2020). Quantifying and understanding the triboelectric series of inorganic non-metallic materials. Nat. Commun. *11*, 2093.

Zou, H.Y., Zhang, Y., Guo, L.T., Wang, P.H., He, X., Dai, G.Z., Zheng, H.W., Chen, C.Y., Wang, A.C., Xu, C., et al. (2019). Quantifying the triboelectric series. Nat. Commun. *10*, 1427.